Kinetics Modelling of CO_2 Chemical Absorption

by

Hardith Singh Mander a/l Ranjeet Singh

15054

Dissertation submitted in partial fulfillment of

the requirements for the

Bachelor of Engineering (Hons)

(Chemical Engineering)

JANUARY 2015

Universiti Teknologi PETRONAS

32610 Bandar Seri Iskandar

Perak Darul Ridzuan

CERTIFICATION OF APPROVAL

Kinetics Modelling of CO_2 Chemical Absorption

by

Hardith Singh Mander a/l Ranjeet Singh

15054

A project dissertation submitted to the
Chemical Engineering Programme
Universiti Teknologi PETRONAS
in partial fulfillment of the requirement for the
BACHELOR OF ENGINEERING (Hons)
(CHEMICAL ENGINEERING)

Approved by,

____

(Dr. Sintayehu Mekuria Hailegiorgis)

UNIVERSITI TEKNOLOGI PETRONAS

JANUARY 2015

CERTIFICATION OF ORIGINALITY

This is to certify that I, Hardith Singh Mander a/l Ranjeet Singh, responsible for the work submitted in this project, that the original work is my own except as specified in the references and acknowledgements, and that the original work contained herein have not been undertaken or done by unspecified sources or persons.

HARDITH SINGH MANDER A/L RANJEET SINGH

ABSTRACT

Natural gas contains high amounts of impurities that are important to remove for commercial usage. One of these impurities are known to be carbon dioxide and it is the main culprit in degrading the gas. It reduces the energy content of natural gas has as well as speeds up corrosion in pipelines and equipment. There are several methods in the removal of this gas one being chemical absorption where the usage of amines are incorporated. In this project, kinetics modelling of blended amine solution of aqueous *N*-methyldiethanolamine (MDEA) and diethanolamine (DEA) were studied where its behavior was simulated using MATLAB. Determining the reaction rate kinetics and the equilibrium constants enabled us the determination of liquid bulk concentration for the overall system. The kinetics at five different temperatures were observed; 303K, 308K, 313K, 318K and 323K for blended amine solution of different MDEA concentrations (1.0 and 1.5 kmol/m3) and DEA concentrations (0.1, 0.2, 0.3 and 0.4 kmol/m3). The Arrhenius relation, activation energy and reaction rate coefficients were obtained showed promising results at three different randomly selected temperatures; 303K, 308K and 323K, where the condition is at its best at 323K at 0.999952193kmol/m3 of MDEA concentration and 0.999912787kmol/ m3 of DEA concentration. This concludes that the kinetic model developed is valid thus can be further enhanced using different and more sophisticated software to ensure best operating conditions for the solution.

ACKNOWLEDGEMENTS

I would like to take this opportunity to express my greatest appreciation to all parties who were involved in finishing my dissertation and Final Year Project and making it a great educational one. I honorably thank University Teknologi PETRONAS and the Chemical Engineering Department for giving me this opportunity to learn and undergo this project which is widely researched in the oil and gas industry. I would also like to thank all for their support and integrity which have played an important role in the success of Final Year Project.

My deepest gratitude also goes to my Supervisor, Dr. Sintayehu Mekuria Hailegiorgis, Lecturer at Chemical Engineering Department, for all his guidance, advice and sharing of his valuable knowledge during the tenure of my Final Year Project. His strength in his knowledge and his years of experience is something that I would really admire and hope to be well-equipped with such skills to be able to apply it in my future. His attention, guidance, willingness and kindness have made the journey of my project a pleasant and successful one.

Last but not least, I would like to thank my family and friends for their never ending support and advice contributing to the successful completion of my Final Year Project.

CONTENTS

CERTIFICATION OF ORIGINALITY ii

ABSTRACT iii

ACKNOWLEDGEMENTS iv

LIST OF FIGURES vii

LIST OF TABLES viii

ABBREVIATION AND NOMENCLATURES ix

CHAPTER 1: INTRODUCTION 1

- 1.1 BACKGROUND 1
- 1.2 PROBLEM STATEMENT 4
- 1.3 OBJECTIVES 5
- 1.4 SCOPE OF STUDY 5

CHAPTER 2: LITERATURE REVIEW 6

- 2.1 METHODS IN CARBON DIOXIDE REMOVAL 6
- 2.2 CARBON DIOXIDE REMOVAL BY ALKANOLAMINES REACTION MECHANISMS 9

CHAPTER 3: METHODOLOGY 11

- 3.1 MODELLING OF EQUATIONS 12
  - 3.1.1 REACTION WITH *N*-METHYLDIETHANOLAMINE (MDEA): 12
  - 3.1.2 REACTION WITH DIETHANOLAMINE (DEA): 13
  - 3.1.3 REACTION WITH WATER ($\boldsymbol{H2O}$): 14
  - 3.1.4 APPARENT RATE CONSTANT FOR $\boldsymbol{CO2}$ ABSORPTION INTO BLENDED AMINE SOLUTION (MDEA +DEA+ H2O): 17
- 3.2 GANTT CHART 19
  - 3.2.1 FYP I 19
  - 3.2.2 FYP II 20

CHAPTER 4: RESULTS AND DISCUSSION 21

- 4.1 ARRHENIUS EQUATION GENERATION USING THE PROPOSED MODEL: 21
  - 4.1.1 Apparent rate of reaction: 21
  - 4.1.2 Determination of $\mathbf{k1}$, $\mathbf{k2}$, $\mathbf{k2(k3/k-2)}$ and $\mathbf{k2(k1/k-2)}$ 24
  - 4.1.3 Determining the rate coefficients at different temperatures 27

4.1.4 Plotting the obtained rate coefficients into Arrhenius Equation......................35
4.2 LIQUID BULK CONCENTRATION ESTIMATION..41
CHAPTER 5: CONCLUSION AND RECOMMENDATION 43
REFERENCES...44
APPENDICES 46

LIST OF FIGURES

Figure 1: World Energy Consumption, 1990- 2035……………………………… 1
Figure 2: Apparent rate constant for the reaction of CO2 with blended amine solution (MDEA: 1.0 kmol/m3) as a function of concentration…………………… 21
Figure 3: Apparent rate constant for the reaction of CO2 with blended amine solution (MDEA: 1.5 kmol/m3) as a function of concentration………………….. 22
Figure 4: Reciprocal of kapp respect to the reciprocal of solution concentration (MDEA:1.0 kmol/m3)………………………………………………………. 23
Figure 5: Reciprocal of kapp respect to the reciprocal of solution concentration (MDEA:1.5 kmol/m3)………………………………………………………. 24
Figure 6: Temperature Dependence of k_2……………………………………... 26
Figure 7: Temperature Dependence of k_1……………………………………... 27
Figure 8: Temperature Dependence of $k_2(k_3/k_{-2})$……………………………… 28
Figure 9: Temperature Dependence of $k_2(k_1/k_{-2})$ …………………………….... 29
Figure 10: Temperature Dependence of k_2 for blended amine solution………… 30
Figure 11: Temperature Dependence of k_1 for blended amine solution………… 31
Figure 12: Temperature Dependence of $k_2(k_3/k_{-2})$ for blended amine solution.. 32
Figure 13: Temperature Dependence of $k_2(k_1/k_{-2})$ for blended amine solution.. 33
Figure 14: $\ln k_2$ versus 1/T…………………………………………………... 36
Figure 15: $\ln k_1$ versus 1/T…………………………………………………... 37
Figure 16: $\ln k_2(k_3/k_{-2})$ versus 1/T…………………………………………….. 38
Figure 17: $\ln k_2(k_1/k_{-2})$ versus 1/T…………………………………………….. 39

LIST OF TABLES

Table 1: Densities and Viscosities of MDEA + MEA + H2O…………………..	7
Table 2: Gantt Chart of FYP I……………………………………………......	18
Table 3: Gantt Chart of FYP II…………………………………………………	19
Table 4: k_{app} of different MDEA and DEA concentrations from (Lin, 2009)…	20
Table 5: Rate coefficient data from MATLAB Simulation……………………..	24
Table 6: Equilibrium Constant…………………………………………………..	40
Table 7: Bulk Concentration……………………………………………………	41

ABBREVIATION AND NOMENCLATURES

MDEA	N-methyldiethanolamine
DEA	Diethanolamine
MEA	Monoethanolamine
CO2	Carbon dioxide
H2O	Water
$\mathrm{k_{app}}$	Apparent rate coefficient between CO2 and blended amine
$\mathrm{k_{ov}}$	Overall reaction
K	Equilibrium constant
k	Rate coefficient of reaction
$\mathrm{X_A}$	Initial CO2 loading

CHAPTER 1: INTRODUCTION

1.1 BACKGROUND

Current world population is estimated to be 7 billion and its increasing rapidly across the globe (Bereau, 2014). Increasing population has indeed resulted in rapid urbanization. This substantial increase directly affects the global energy consumption which causes it to increase to meet global energy demand. The overall world energy demand is estimated to increase from 505 quadrillion BTU in the year 2008 to 770 quadrillion BTU in 2035 (Administration, 2014) as shown in the figure below:

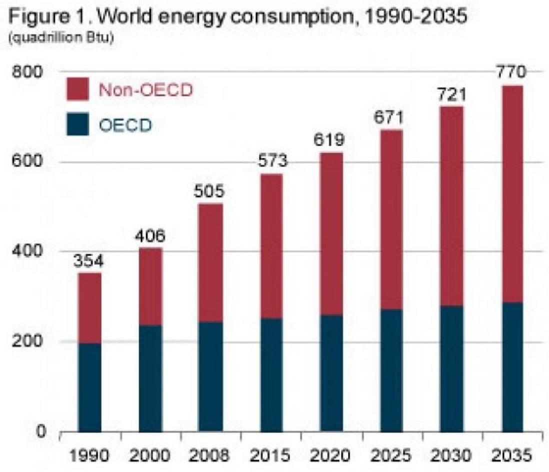

Figure 1: World Energy Consumption, 1990- 2035

About 80.7% of the world’s energy consumption is based on fossil fuels (Eyton, 2014). When these fossil fuels are combusted, they release harmful byproducts into the atmosphere. There are known to be three types of fossil fuels; oil, coal and natural gas. In combustion, the burning of those three fossil fuels, produces high amount of carbon dioxide that pollutes the environment and increases the surrounding temperature. Although, carbon dioxide is a naturally occurring compound found in air with a total composition of 0.03%, this gas, when produced in abundance, it contributes to global warming. It is one of the many greenhouse gases that aids in this phenomenon.

Natural gas is a combustible mixture of hydrocarbon gases which is known to be colourless as well as odourless. This gas is known to produce high amount of energy and serves as a vital component of the world's supply of energy. Natural gas in Malaysia naturally contains high amount of carbon dioxide which can range from 20% (Bergading Platform) (Ali, 2010) to 66% (Bujang Field) (Ismail, 2010) or more. High percentage of CO2 can aid in corrosion of pipelines and equipment in a plant which could result in accidents and loss of lives. It also reduces the calorific value of the fuel gas which makes it less combustible and has no value in the market. Therefore, this gas has to be removed to level where it is optimum for usage which is approximately 0-8%. In order to obtain a percentage that is significantly low, several processes that aids in the removal of CO2 can be conducted. Processes such as chemical absorption, cryogenic, adsorption and membrane system are widely used in the oil and gas industry for the removal of CO2 from natural gas.

Membrane separation works according to the principle of selective permeation which occurs through a membrane surface. In a membrane system, membrane modules are pressurized with a gas mixture where the differential in pressure and concentration, known to be the driving force in this process, separates the gas components (Cameron, 2013). This technique has increased awareness in the importance of CO2 removal but due to its nature of causing a fouling and plugging effect, high hydrocarbon losses are observed and a high cost involved in recovering the hydrocarbon through another system (Yan et al., 2008).

Another method called cryogenic uses a turbo expander. It is a gas turbine that is driven by the expanding gas which then cools to below the dew point for the gas to be removed. This method is often used when the content of CO2 is high, approximately more than 50mole% which limits its usage in the oil and gas industry for CO2 removal.

Adsorption is a method where it relies on the gas molecules that contain acid gas to bind to the surface of a specific solid. The acid gas is then released by regeneration after a certain time. There are several principles involved in order for this process to work effectively:

- Pressure Swing Adsorption (PSA)
- Temperature Swing Adsorption (TSA)
- Electric Swing Adsorption (ESA) (Grande & Rodrigues, 2008)

Unfortunately, this method of removal is suitable for large scale separation of CO2. Reason being the capacity and CO2 selectivity of the pre-existing adsorbents is low (Joel Toreja, 2011).

Chemical absorption is used to reduce the concentration of carbon dioxide in natural gas by diffusing into the interior of amorphous solid or liquids in a solvent. In this system, aqueous alkanolamines solutions are commonly used as solvents to aid in the removal of this acidic gas. Alkanolamines such as monoethanolamine (MEA), di-isopropanolamine (DIPA), triethanolamine (TEA), *N*-methyldiethanolamine (MDEA), 2-amino-2methyl-1-propanol (AMP), and 2-piperidineethanol (2-PE) can act as an absorbent in the process of acid gas removal (Kohl & Nielsen, 1997). Blended amine solutions where aqueous solutions of MEA + MDEA (Liao & Li, 2002) and MDEA + DEA (Lin, Soriano, & Li, 2009) are suggested to be used in this system of acid gas absorption. This method is advised rather than using it individually because the addition of small amounts of primary amine to conventional tertiary amines can enhance the absorption rate of CO2 in the gas stream (Liao & Li, 2002).

1.2 PROBLEM STATEMENT

Reserves that are particularly located in North Malay Basin, Sabah and Sarawak are found to contain high compositions of carbon dioxide in raw natural gas. Generally, the composition of carbon dioxide ranges from 20% (Bergading Platform) to 66% (Bujang Field) in the North Malay Basin and 47% (Tenggiri Mrn.) to 87% (J5 platform) in Sarawak (Ali, 2010). Current technology available using cryogenic, adsorption and membrane system available is only limited to either removal of high CO2 concentration, bulk removal of CO2 or its nature of causing a fouling and plugging effect which contributes to hydrocarbon losses. In chemical absorption, the use of primary or secondary amine (MEA or DEA) as a solvent in removal of CO2 is undesirable as its loading capacity is fixed to a maximum of 0.5 mole of CO2 per mole of amine (Arthur J. Kidnay, 2006) whereas tertiary amines (MDEA) are able to achieve up to 1 mole of CO2 loading per mole of amines but has a downside of slow absorption rate. However, there are several properties that make MDEA attractive for the absorption of CO2. This tertiary amine is known to have a high solution concentration which ranges up to 50-55wt%, high acid gas loading, low corrosion although the solution holdings are high, lower heats of reaction and low vapor pressure and solution losses (Jerry A. Bullin, 1990). Therefore, addition of small amounts of primary amine or secondary amine into the MDEA solution, significantly enhances the CO2 absorption rate (Liao & Li, 2002). MEA offer significantly low selectivity in normal operating units whereas DEA and MDEA are selective amines which known to be more effective at high pressures, approximately more than 300 psi (Kevin M. Lunsford, 1996). Blends of these amines are desirable because it combines the high absorption capacity of MDEA with the high absorption rates with MEA and DEA (Zhang, Schubert, Gruenewald, & Agar, 2005). A new approach will be conducted in order to improve the CO2 absorption into the blended amine solutions by obtaining the kinetics pertaining to this mixture thus varying the concentrations of the secondary amine and tertiary amine. The performance of this system in absorbing CO2 from the raw natural gas is to be further studied via modelling and simulation using MATLAB.

1.3 OBJECTIVES

1. To screen and identify mathematical models that involves in the absorption kinetics of CO2 removal in the blended amine solution.
2. To use the developed model to estimate the kinetic rate coefficient of the blended amine solution.
3. To calculate the Arrhenius equation of the blended amine solution.
4. To simulate and obtain the liquid bulk concentrations based on the past literatures correlation.

1.4 SCOPE OF STUDY

This research project is focused on developing the reactive absorption kinetics of carbon dioxide removal in a blended aqueous amine solution of diethanolamine (DEA) and methyldiethanolamine (MDEA). Various alkanolamines are able to act as a solvent in reducing the concentration of carbon dioxide in gas streams. However, each alkanolamine has its own preference in determining the solubility and diffusivity of CO2. In order to enhance the process, addition of small amounts of primary amine or secondary amine are added into conventional tertiary amines (Liao & Li, 2002). Primary amines like monoethanolamine (MEA), offer significantly low selectivity in normal operating units whereas secondary and tertiary amines such as diethanolamine (DEA) and *N*-methyldiethanolamine are selective amines which known to be more effective at high pressures (Kevin M. Lunsford, 1996). Therefore, several literature studies will be a key in determining the best mathematical model for the reactive absorption of CO2. Modelling of the kinetics behavior and simulation processes will be done using MATLAB.

CHAPTER 2: LITERATURE REVIEW

2.1 METHODS IN CARBON DIOXIDE REMOVAL

There are different type of processes involved in the removal of carbon dioxide from a gas stream. As mentioned in Chapter 1, methods such as chemical absorption, adsorption and membrane system are well known in this removal process. Putting aside the other methods, chemical absorption using alkanolamines has conventionally and economically been used in the oil and gas industry. Ways in such as only primary amines are used as solvents or a mixture of primary and tertiary amines only determines the rate of absorption of CO2 in the solvent.

Recent studies has been carried out by understanding the kinetics of absorption of CO2 into aqueous *N*- methyldiethanolamine (MDEA + H2O). The absorption of CO2 has been conducted at three different temperatures using a laboratory wetted column and four different concentrations of MDEA, 1.0, 1.5, 2.0, 2.5 kmol m^{-3}. The N2O analogy was used to understand the solubility and diffusivity of CO2 in the solution (Ko & Li, 2000). The second order-rate constant of CO2 in MDEA was found to be as:

$$\frac{\mathrm{k}_{2,\mathrm{MDEA}}}{\mathrm{m}^3\mathrm{kmol}^{-1}\mathrm{s}^{-1}} = 4.01 \times 10^8 \exp[-\frac{5400}{\mathrm{T(K)}}]$$

Therefore, the activation energy was found to be 44.9 kJmol^{-1} (Ko & Li, 2000). This result is proven to be satisfactory compared to other studies conducted for temperatures from 20°C to 80°C (Ko & Li, 2000).

Other studies involving blended amine solutions has also been carried out where primary amines are mixed with tertiary amines to enhance the solubility and diffusivity of CO2. Kinetics of absorption of CO2 in monoethanolamine and *N*- methyldiethanolamine (MDEA + MEA) were investigated where the MEA concentrations of 0.1, 0.2, 0.3, 0.4 and 0.5 kmol m^{-3} were mixed with MDEA concentrations of 1.0 and 1.5 kmol m^{-3} (Liao & Li, 2002). The density of the overall solution increases as the concentration of MEA increases. Moreover, the increase in temperature has resulted in decrease in density as shown in Table 1:

Table 1: Densities and Viscosities of MDEA + MEA + H2O

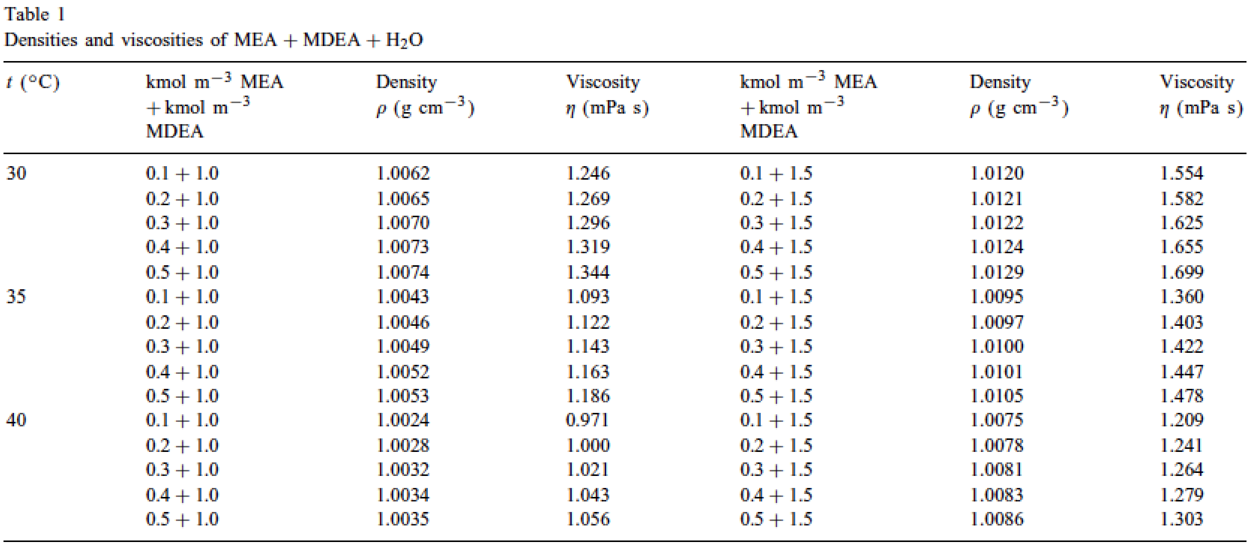

Table 1
Densities and viscosities of MEA + MDEA + H_2O

t (°C)	kmol m^{-3} MEA + kmol m^{-3} MDEA	Density ρ (g cm^{-3})	Viscosity η (mPa s)	kmol m^{-3} MEA + kmol m^{-3} MDEA	Density ρ (g cm^{-3})	Viscosity η (mPa s)
30	0.1 + 1.0	1.0062	1.246	0.1 + 1.5	1.0120	1.554
	0.2 + 1.0	1.0065	1.269	0.2 + 1.5	1.0121	1.582
	0.3 + 1.0	1.0070	1.296	0.3 + 1.5	1.0122	1.625
	0.4 + 1.0	1.0073	1.319	0.4 + 1.5	1.0124	1.655
	0.5 + 1.0	1.0074	1.344	0.5 + 1.5	1.0129	1.699
35	0.1 + 1.0	1.0043	1.093	0.1 + 1.5	1.0095	1.360
	0.2 + 1.0	1.0046	1.122	0.2 + 1.5	1.0097	1.403
	0.3 + 1.0	1.0049	1.143	0.3 + 1.5	1.0100	1.422
	0.4 + 1.0	1.0052	1.163	0.4 + 1.5	1.0101	1.447
	0.5 + 1.0	1.0053	1.186	0.5 + 1.5	1.0105	1.478
40	0.1 + 1.0	1.0024	0.971	0.1 + 1.5	1.0075	1.209
	0.2 + 1.0	1.0028	1.000	0.2 + 1.5	1.0078	1.241
	0.3 + 1.0	1.0032	1.021	0.3 + 1.5	1.0081	1.264
	0.4 + 1.0	1.0034	1.043	0.4 + 1.5	1.0083	1.279
	0.5 + 1.0	1.0035	1.056	0.5 + 1.5	1.0086	1.303

From the experiment, it is concluded that the addition of small amounts of MEA into the MDEA has resulted in significant higher absorption rates of CO2 and the model is satisfactory (Liao & Li, 2002).

Blended amine solutions using diethanolamine and *N*- methyldiethanolamine (MDEA + DEA) study has also been carried out where DEA concentrations of 0.1, 0.2, 0.3, and 0.4 $kmol\ m^{-3}$ were mixed with MDEA concentrations of 1.0 and 1.5 $kmol\ m^{-3}$ (Lin et al., 2009). It is proven from this experiment that the addition of small amounts of DEA into the MDEA resulted in a significant enhancement of CO2 absorption rates (Lin et al., 2009). Besides that, it is also mentioned that the reaction between CO2 and MDEA is a pseudo first-order reaction as follows (Blauwhoff, Versteeg, & Van Swaaij, 1984):

$$\mathrm{r_{CO_2-MDEA} = k_{2,MDEA}[CO_2][MDEA]}$$

Where $\mathrm{k_{2,MDEA}}$ is the pseudo first-order constant, [CO2] and [MDEA] (Lin et al., 2009).

2.2 CARBON DIOXIDE REMOVAL BY ALKANOLAMINES REACTION MECHANISMS

As mentioned in Chapter 1, there are several types of alkanolamines that can be used for carbon dioxide absorption. Amines such as monoethanolamine (MEA), di-isopropanolamine (DIPA), triethanolamine (TEA), *N*-methyldiethanolamine (MDEA), 2-amino-2methyl-1-propanol (AMP), and 2-piperidineethanol (2-PE) can be used as a solvent in CO2 absorption.

Throughout the years, MDEA has be known to take advantage of its capability of selective absorption. Unfortunately, MDEA is well known for its relatively low CO2 absorption rate. From this study, it has concluded that MDEA is not usually associated when it involves large amounts of CO2. But on the other hand, there are several properties that make MDEA attractive for the absorption of CO2. It has a high solution concentration which ranges up to 50-55wt%, high acid gas loading, low corrosion although the solution holdings are high, lower heats of reaction and low vapor pressure and solution losses (Jerry A. Bullin, 1990). Below shows the reaction mechanism of carbon dioxide with MDEA (Lin et al., 2009):

$$\mathrm{CO_2 + R_3N + H_2O \leftrightarrow R_3NH^+ + HCO_3^-}$$

The previous reaction shows that it is a base-catalyzed hydration of CO2. Therefore, it is proven that tertiary amines are not able to react directly with carbon dioxide (Blauwhoff et al., 1984). According to (Lin et al., 2009), there are two types of reactions that will occur for CO2 in aqueous solutions:

First: Hydration of CO2

$$\mathrm{CO_2 + H_2O \leftrightarrow HCO_3^- + H^+}$$

Second: Bicarbonate formation

$$\mathrm{CO_2 + OH^- \leftrightarrow HCO_3^-}$$

The first reaction is usually neglected (Blauwhoff et al., 1984) whereas the second reaction is considerably fast and can enhance the mass transfer although when the hydroxyl concentration considered to be low (Lin et al., 2009).

Adding on to the advantages of MDEA, addition of small amounts of primary amine or secondary amine into the MDEA solution, significantly enhances the CO2 absorption rate (Liao & Li, 2002). Primary amines like monoethanolamine (MEA), offer significantly low selectivity in normal operating units whereas secondary and tertiary amines such as diethanolamine (DEA) and *N*- methyldiethanolamine are selective amines which known to be more effective at high pressures, approximately more than 300 psi (Kevin M. Lunsford, 1996). Therefore, it is concluded that the blends of primary amines or secondary amines with the tertiary amine because it combines the high absorption capacity of MDEA with the high absorption rates with MEA and DEA (Zhang et al., 2005).

CHAPTER 3: METHODOLOGY

First task that has to be conducted in order to proceed with this project is to gather information regarding the proposed topic. From the topic, certain keywords are extracted such as kinetic modelling, chemical absorption and CO2 removal. These keywords are used in order to search for literature reviews and past journals that has any relation to kinetics modelling of CO2 removal using chemical absorption. Extensive research was conducted and several literatures has been discovered. Understanding each literature was a crucial task as it requires adequate attention and commitment.

Different literatures show different approaches towards a particular method. Each method were thoroughly studied by taking in account of the mathematical models and parameters in which the research has been conducted. From the study of literatures, reaction kinetics equation between carbon dioxide and the blended amine solution will be developed. Parameters involved such as the temperature and concentration of amines will be evaluated as well as estimating the rate constant of the overall process. Further study will be done through simulation by using a modelling software which is feasible for this study; MATLAB. Thus the model will be validated by comparing to the results obtain from past literatures. Finally, the model will then be able to determine the best operating conditions for the absorption of carbon dioxide.

3.1 MODELLING OF EQUATIONS

There are three types of reactions that occur in the blended amine solution of aqueous *N*-methyldiethanolamine (MDEA) and diethanolamine (DEA). Each of this species undergoes a reaction with the carbon dioxide, water as well as the amines itself. Below shows the step-by-step reaction mechanism between those reactions thus enabling the model equation to be developed. In the mechanisms below, $\mathrm{K_A}$ is represented as the equilibrium constant, $\mathrm{k_A}$ as the forward rate coefficient and $\mathrm{k_{-A}}$ as the reverse rate coefficient; where A is denoted as the reaction number.

3.1.1 REACTION WITH *N*-METHYLDIETHANOLAMINE (MDEA):

The reaction with *N*-methyldiethanolamine (MDEA) is basically hydration of carbon dioxide with MDEA acting as a catalyst. The reaction below shows the reaction mechanism between carbon dioxide (CO_2) and aqueous MDEA (R_3N) which results in a pseudo first order reaction.

$$\mathrm{CO_2 + R_3N + H_2O \xleftrightarrow{K_1,k_1,k_{-1}} R_3NH^+ + HCO_3^-} \tag{1}$$

Pseudo first order reaction:

$$\mathrm{r_{CO_2-MDEA} = k_{2,MDEA}[CO_2][MDEA]}$$

3.1.2 REACTION WITH DIETHANOLAMINE (DEA):

The reaction below represents the reaction between carbon dioxide and diethanolamine which are represented by CO_2 and R_1R_2NH respectively.

$$CO_2 + R_1R_2NH \xleftrightarrow{K_2,k_2,k_{-2}} R_1R_2NH^+COO^- \tag{2}$$

$$R_1R_2NH^+COO^- + R_1R_2NH \xleftrightarrow{K_3,k_3,k_{-3}} R_1R_2NH_2^+ + R_1R_2NCOO^- \tag{3}$$

Reaction (3) shows the formation of a zwitterion ($R_1R_2NH^+COO^-$) where it contains both positive and negative ions. Thus, the DEA will be taken as the only base that deprotonates this zwitterion. The forward reaction rate at quasi-steady state:

$$r_{CO_2-DEA} = \frac{k_{2,DEA}[CO_2][DEA]}{1 + k_{-1}/(k_{H_2O}[H_2O] + k_{OH^-}[OH^-] + k_{DEA}[DEA] + k_{MDEA}[MDEA])}$$

Furthermore, deprotonation of zwitterion also occurs when reacted with water, hydroxide ion and bicarbonate ion which are known to be reversible with finite reaction rates as shown as in the reactions below. Besides that, some reactions are also known to be instantaneous as well as reversible. This is because these reactions only involve the transfer of protons. Reactions are shown as below:

$$R_1R_2NH^+COO^- + H_2O \xleftrightarrow{K_4,k_4,k_{-4}} H_3O^+ + R_1R_2NCOO^- \tag{4}$$

$$R_1R_2NH^+COO^- + OH^- \xleftrightarrow{K_5,k_5,k_{-5}} H_2O + R_1R_2NCOO^- \tag{5}$$

$$R_1R_2NH^+COO^- + HCO_3^- \xleftrightarrow{K_6,k_6,k_{-6}} H_2CO_3 + R_1R_2NCOO^- \tag{6}$$

$$R_1R_2NH^+COO^- + CO_3^{2-} \xleftrightarrow{K_7,k_7,k_{-7}} HCO_3^- + R_1R_2NCOO^- \tag{7}$$

$$R_1R_2NCOO^- + H_2O \xleftrightarrow{K_8,k_8,k_{-8}} HCO_3^- + R_1R_2NH \tag{8}$$

$$R_1R_2NH_2^+ + OH^- \overset{K_9}{\leftrightarrow} H_2O + R_1R_2NH \tag{9}$$

$$HCO_3^- + OH^- \overset{K_{10}}{\longleftrightarrow} H_2O + CO_3^{2-} \tag{10}$$

$$2H_2O \overset{K_{11}}{\longleftrightarrow} H_3O^+ + OH^- \tag{11}$$

$$HCO_3^- + H_3O^+ \overset{K_{12}}{\longleftrightarrow} H_2O + H_2CO_3 \tag{12}$$

3.1.3 REACTION WITH WATER (H_2O):

Generally, there are two types of reaction that occurs for carbon dioxide in aqueous solution; Hydration of CO_2 and Bicarbonate Formation:

$$CO_2 + OH^- \xleftrightarrow{K_{13},k_{13}} HCO_3^- \tag{13}$$

$$CO_2 + H_2O \xleftrightarrow{K_{14},k_{14}} H_2CO_3 \tag{14}$$

Hydration of CO2 (14) is often neglected as its reaction is very slow (Blauwhoff et al., 1984). Therefore, the second reaction is considered as it is fast and can enhance mass transfer although the OH^- concentration is low. Forward reaction with H_2O is described as:

$$r_{CO_2-OH^-} = k^*_{OH^-}[CO_2][OH^-]$$

Assumptions are made in this project in order to determine the liquid bulk concentration of each chemical species. This can be determined from the initial concentrations of the blended amine solution, the initial carbon dioxide loading, X_A and assuming that the reactions are at equilibrium. Each of the chemical species has be renamed for better understanding on the system where as liquid bulk concentration are denoted to be C'_{A} and so on:

$\mathrm{C_A} = [\mathrm{R_3N}]$
$\mathrm{C_B} = [\mathrm{R_3NH^+}]$
$\mathrm{C_C} = [\mathrm{R_1R_2NH}]$
$\mathrm{C_D} = [\mathrm{R_1R_2NH_2^+}]$
$\mathrm{C_E} = [\mathrm{R_1R_2NCOO^-}]$
$\mathrm{C_F} = [\mathrm{CO_2}]$
$\mathrm{C_G} = [\mathrm{HCO_3^-}]$
$\mathrm{C_H} = [\mathrm{OH^-}]$
$\mathrm{C_I} = [\mathrm{CO_3^{2-}}]$
$\mathrm{C_J} = [\mathrm{H_3O^+}]$
$\mathrm{C_K} = [\mathrm{H_2CO_3}]$
$\mathrm{C_L} = [\mathrm{H_2O}]$

Overall $\mathrm{R_3N}$ balance:

$$\mathrm{C'_A} + \mathrm{C'_B} = [\mathrm{R_3N}]_{initial} \tag{15}$$

Overall $\mathrm{R_1R_2NH}$ balance:

$$\mathrm{C'_C} + \mathrm{C'_D} + \mathrm{C'_E} = [\mathrm{R_1R_2NH}]_{initial} \tag{16}$$

Overall carbon dioxide balance:

$$\mathrm{C'_F} + \mathrm{C'_G} + \mathrm{C'_I} + \mathrm{C'_E} + \mathrm{C'_K} = \mathrm{X_A}\{[\mathrm{R_3N}]_{initial} + [\mathrm{R_1R_2NH}]_{initial}\} \tag{17}$$

Overall electroneutrality balance:

$$\mathrm{C'_B} + \mathrm{C'_D} + \mathrm{C'_J} - \mathrm{C'_G} - \mathrm{C'_H} - 2\mathrm{C'_I} - \mathrm{C'_E} = 0 \tag{18}$$

Hence, the equilibrium constants are as per below:

$$\mathrm{K_1} = \frac{\mathrm{C'_B C'_G}}{\mathrm{C'_A C'_F C'_L}} \tag{19}$$

$$\mathrm{K_2 K_3 K_9 K_{11}} = \frac{\mathrm{C'_E C'_J}}{\mathrm{C'_C C'_F}} \tag{20}$$

$$\mathrm{K_9} = \frac{\mathrm{C'_C}}{\mathrm{C'_D C'_H}} \tag{21}$$

$$K_{10} = \frac{C'_I}{C'_G C'_H} \tag{22}$$

$$K_{11} = C'_H C'_J \tag{23}$$

$$K_{12} = \frac{C'_K}{C'_G C'_J} \tag{24}$$

$$K_{13} = \frac{C'_G}{C'_F C'_H} \tag{21}$$

In determining the model for the overall system, certain reactions has been considered as well as neglected by abiding to some terms and conditions. Reactions (6) and (7) are neglected as the bicarbonate and carbonate in the aqueous solution are low. Moreover, the deprotonation of the zwitterions contribution in the system is very low so therefore it is considered as negligible. These modifications were made based on the assumptions that the gas-liquid contact times was very short. Another assumption was made when hydroxide concentration is very low, it is difficult to quantify the hydroxide contribution to the deprotonation of the zwitterions thus enabling reaction (5) to be eliminated.

In this project, DEA will be taken as the only base that deprotonates this zwitterion. Hence, any other reactions that involves water to deprotonate the zwitterions are neglected. This includes reactions (4), (5), (6), (7) and (8).

3.1.4 APPARENT RATE CONSTANT FOR CO_2 ABSORPTION INTO BLENDED AMINE SOLUTION (MDEA +DEA+ H2O):

Overall reaction:

$$r_{ov} = r_{CO_2-MDEA} + r_{CO_2-DEA} + r_{CO_2-OH^-}$$

$$\begin{aligned}
&k_{ov}\\
&= k_{2,MDEA}[MDEA] + k^{*}_{OH^-}[OH^-]\\
&+ \frac{[DEA]}{\left(\frac{1}{k_{2,DEA}}\right) + \frac{1}{\left(\left(\frac{k_{2,DEA}k_{H_2O}}{k_{-1}}\right)[H_2O] + \left(\frac{k_{2,DEA}k_{OH^-}}{k_{-1}}\right)[OH^-] + \left(\frac{k_{2,DEA}k_{DEA}}{k_{-1}}\right)[DEA] + \left(\frac{k_{2,DEA}k_{MDEA}}{k_{-1}}\right)[MDEA]\right)}}
\end{aligned}$$

Apparent reaction rate constant:

$$k_{app} = k_{ov} - k^{*}_{OH^-}[OH^-]$$

Therefore,

$$k_{app} = k_{2,MDEA}[MDEA] + \frac{[DEA]}{\left(\frac{1}{k_{2,DEA}}\right) + \frac{1}{\left(\left(\frac{k_{2,DEA}k_{DEA}}{k_{-1}}\right)[DEA] + \left(\frac{k_{2,DEA}k_{MDEA}}{k_{-1}}\right)[MDEA]\right)}}$$

Hence, substituting the terms into the above equation yields:

$$\frac{1}{k_{app}} = \frac{1}{k_1} + \frac{1}{k_2} + \frac{1}{k_2(k_3/k_{-2})C_C} + \frac{1}{k_2(k_1/k_{-2})C_A} \qquad (22)$$

The correlations used for the equilibrium constant estimation (Mandal, 2003) and (Lin, 2009) are shown as per below:

$$\log_{10}(\mathrm{K}_{13})\left(\frac{\mathrm{m}^3}{(\mathrm{kmol\ s})}\right) = 13.635 - \frac{2895}{\mathrm{T(K)}}$$

$$\log_{10}(1/\mathrm{K}_9)\left(\frac{\mathrm{m}^3}{(\mathrm{kmol\ s})}\right) = -4.0302 - \frac{18.30.15}{\mathrm{T(K)}} + 0.0043 * \mathrm{T}$$

$$\log_{10}(\mathrm{K}_{10})\left(\frac{\mathrm{m}^3}{(\mathrm{kmol\ s})}\right) = 6.498 - \frac{2902.4}{\mathrm{T(K)}} - 0.0238 * \mathrm{T}$$

$$\log_{10}(1/\mathrm{K}_{11})\left(\frac{\mathrm{m}^3}{(\mathrm{kmol\ s})}\right) = 8909.48 - \frac{142613.6}{\mathrm{T(K)}} - 4229.2 * \log_{10}(T) + 9.738 * T$$

3.2 GANTT CHART

3.2.1 FYP I

Table 2: Gantt Chart of FYP I

No.	Task/ Week	1	2	3	4	5	6	7	8	9	10	11	12	13	14
1	Project Title Selection	🟥	🟥												
2	Journals and Literature Research		🟥	🟥	🟥	🟥	🟥	🟥							
3	Submission of Extended Proposal							🟦							
4	Proposal Defense Presentation								🟥						
5	Continuation of Project Work									🟥	🟥	🟥	🟥		
6	Interim Draft Report Submission												🟦	🟦	
7	Interim Report Submission														🟦

🟥 Process

🟦 Milestone

3.2.2 FYP II

Table 3: Gantt Chart of FYP II

No.	**Task/ Week**	**1**	**2**	**3**	**4**	**5**	**6**	**7**	**8**	**9**	**10**	**11**	**12**	**13**	**14**
1	Simulation Work Part 1	🟥	🟥	🟥	🟥	🟥	🟥	🟥							
2	Progress Report Submission								🟦						
3	Simulation Work Part 2								🟥	🟥	🟥	🟥	🟥		
4	Submission of Draft Report												🟦		
5	Continuation of Project Work												🟥	🟥	🟥
6	Softbound Submission													🟦	
7	Oral Presentation														🟦

🟥	Process
🟦	Milestone

CHAPTER 4: RESULTS AND DISCUSSION

4.1 ARRHENIUS EQUATION GENERATION USING THE PROPOSED MODEL:

4.1.1 APPARENT RATE OF REACTION:

Apparent rate of reaction quantifies the overall reaction rate between carbon dioxide and the blended amine solution. The apparent rate of reaction in this study is obtained from past literature (Lin, 2009) where it is stated below for each concentration of MDEA and DEA:

Table 4: $\mathrm{k_{app}}$ of different MDEA and DEA concentrations from (Lin, 2009)

MDEA (kmol/m3) + DEA (kmol/m3)	$\mathrm{k_{app}}/s^{-1}$
1.0 + 0.1	77.6
1.0 + 0.2	151.2
1.0 + 0.3	253.0
1.0 + 0.4	363.0
1.5 + 0.1	103.3
1.5 + 0.2	227.8
1.5 + 0.3	342.4
1.5 + 0.4	530.9

With the obtained values from the Table 4, graphs of Figure 2 and Figure 3 of kapp are plotted against the different DEA concentrations of 0.1, 0.2 0.3 and 0.4 kmol/m3. The current line shows that a 10% in increment in kapp has been made on the previous study since there are no experimental data for the blended amine solution. The current line shows the trend that will be exhibited from the increment mentioned from the past literature data.

Figure 2 shows the trend exhibited by MDEA at concentration of 1.0 kmol/m3 whereas Figure 3 shows for MDEA at concentration of 1.5 kmol/m3 using MATLAB.

(MDEA: 1.0 kmol/m3)

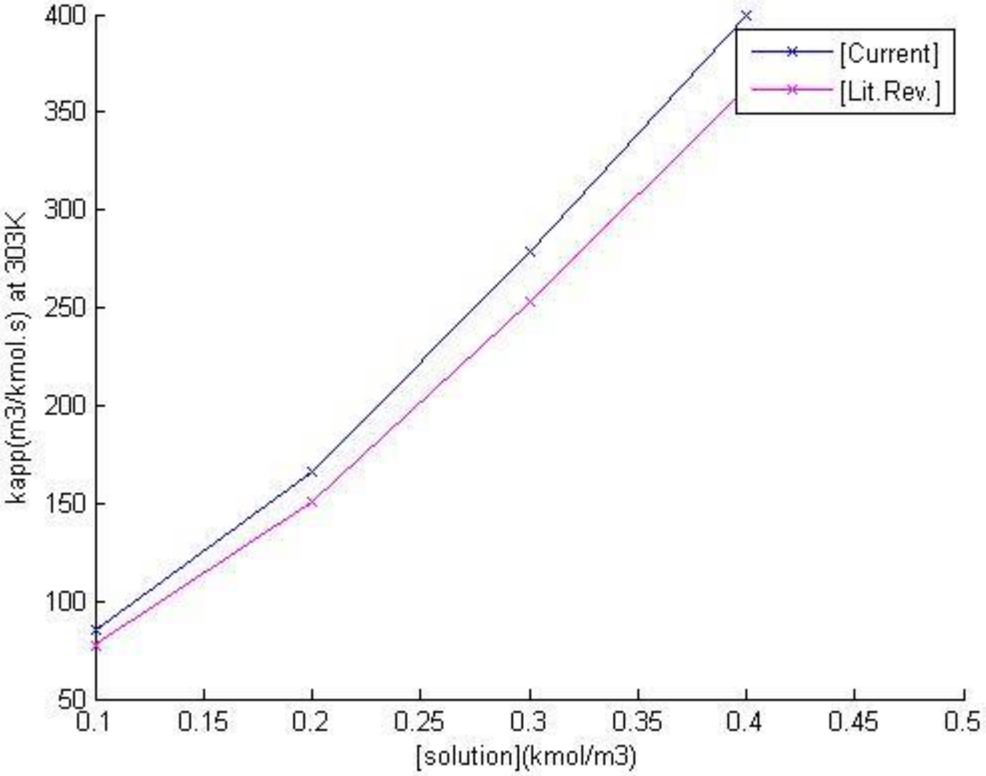

Figure 2: Apparent rate constant for the reaction of CO2 with blended amine solution (MDEA: 1.0 kmol/m3) as a function of concentration.

(MDEA: 1.5 kmol/m3)

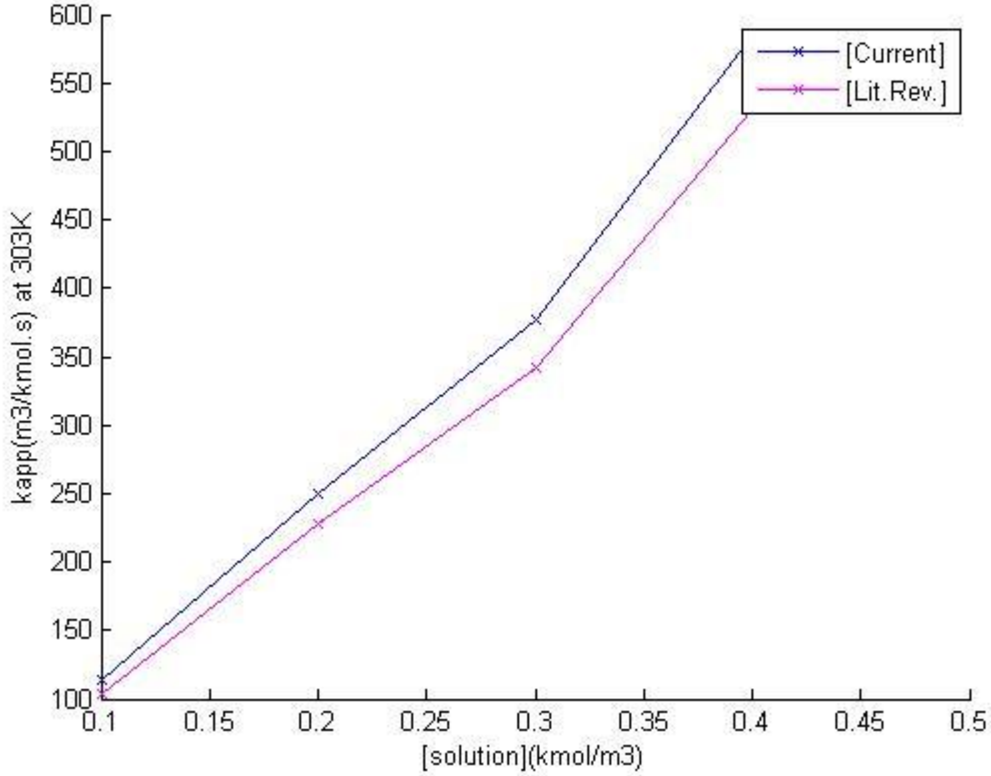

Figure 3: Apparent rate constant for the reaction of CO2 with blended amine solution (MDEA: 1.5 kmol/m3) as a function of concentration.

From the trend observed from Figure 2 and Figure 3, the forward and reverse rate coefficient of reaction will be determined by plotting the reciprocal of kapp against the reciprocal of DEA concentrations.

4.1.2 DETERMINATION OF $\mathbf{k_1}$, $\mathbf{k_2}$, $\mathbf{k_2(k_3/k_{-2})}$ AND $\mathbf{k_2(k_1/k_{-2})}$.

Reciprocal of kapp respect to the reciprocal of DEA concentrations of 0.1, 0.2, 0.3 and 0.4 kmol/m3 are plotted as in Figure 4 and Figure 5. It also shows the comparison with the results obtained from past literature and from Figure 2 and Figure 3. This enables values of forward and reverse reactions of the blended amine solution to be easily determined by using y = mx + c. Figure 4 shows the trend exhibited by MDEA at concentration of 1.0 kmol/m3 whereas Figure 5 shows for MDEA at concentration of 1.5 kmol/m3 using MATLAB.

(MDEA: 1.0 kmol/m3)

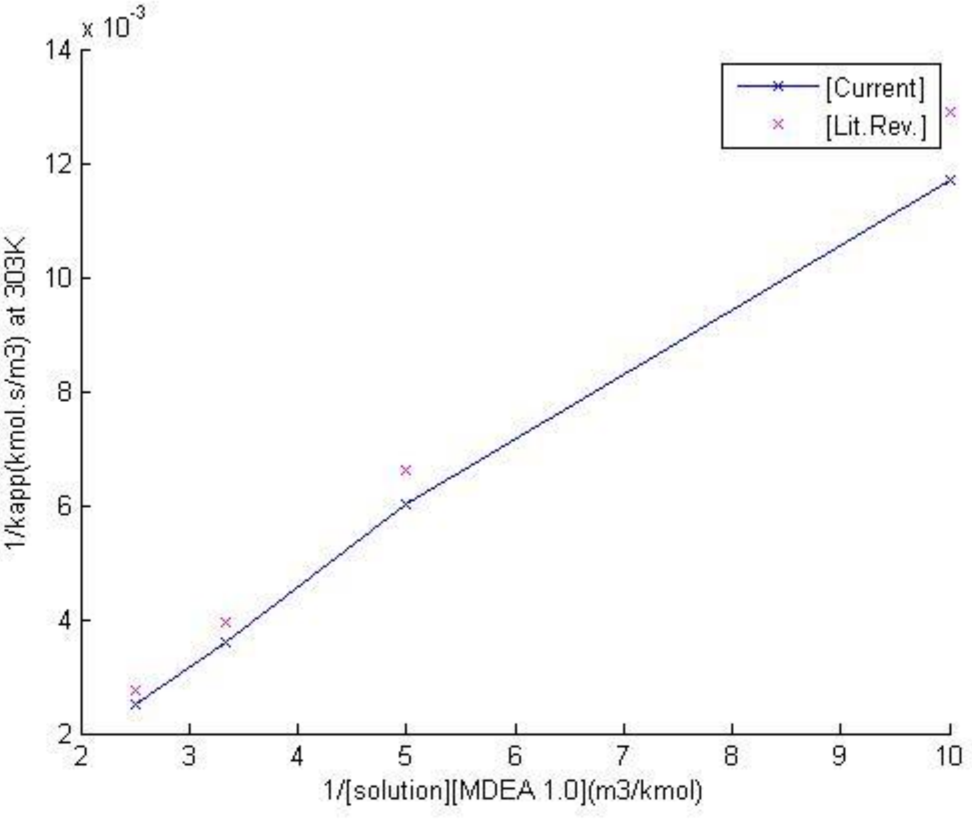

Figure 4: Reciprocal of kapp respect to the reciprocal of solution concentration (MDEA:1.0 kmol/m3)

(MDEA: 1.5 kmol/m3)

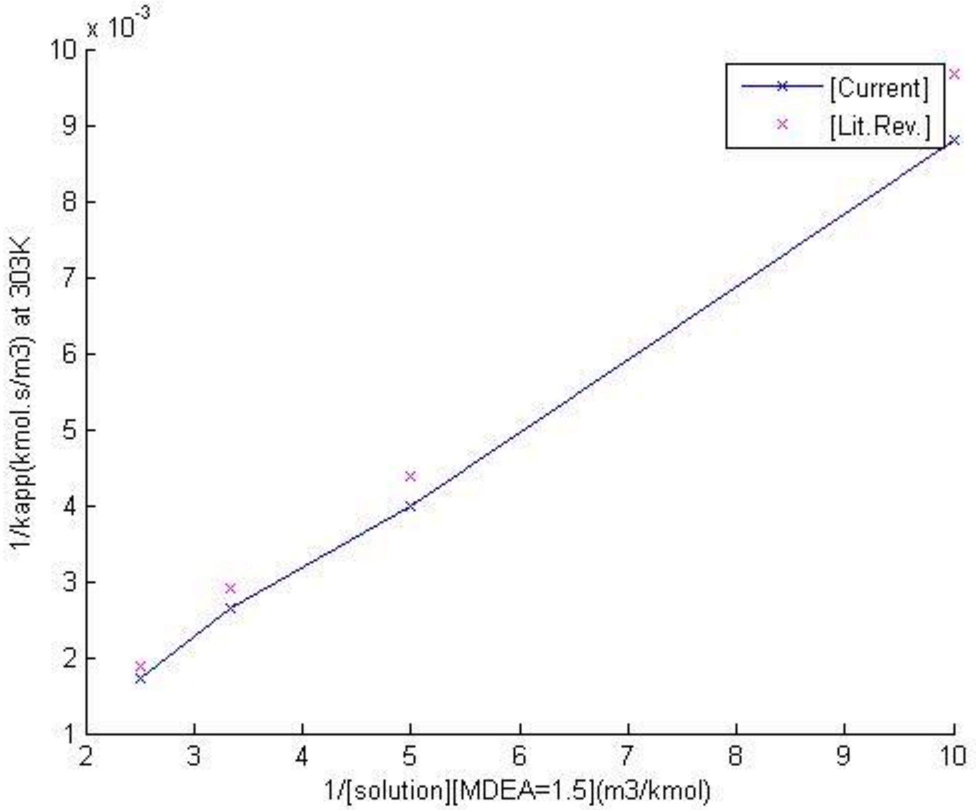

Figure 5: Reciprocal of kapp respect to the reciprocal of solution concentration (MDEA:1.5 kmol/m3)

The graphs of Figure 4 and Figure 5 are plotted using the developed equation (22) using MATLAB simulation as shown as below:

$$\frac{1}{k_{app}} = \frac{1}{k_1} + \frac{1}{k_2} + \frac{1}{k_2(k_3/k_{-2})C_C} + \frac{1}{k_2(k_1/k_{-2})C_A}$$

From the equation (22), it is known to be linear where it will be in terms of y= mx+c:

$\frac{1}{\mathrm{k}_1}+\frac{1}{\mathrm{k}_2}=\mathrm{c}\ (\mathrm{y}-\mathrm{intercept})$, while $\frac{1}{\mathrm{k}_2(\mathrm{k}_3/\mathrm{k}_{-2})}+\frac{1}{\mathrm{k}_2(\mathrm{k}_1/\mathrm{k}_{-2})}=\mathrm{m}\ (\mathrm{gradient})$

The values of m obtained from the gradient of Figure 4 and Figure 5 at 303K are:

MDEA: 1.0 kmol/m3 = 0.0012218

MDEA: 1.5 kmol/m3 = 0.00093701

By solving the equation simultaneously, it is calculated that the values of:

$$\frac{1}{\mathrm{k}_2(\mathrm{k}_3/\mathrm{k}_{-2})}=3.588\times 10^{-4} kmol^2.s/m^6$$

Hence,

$$\mathrm{k}_2(\mathrm{k}_3/\mathrm{k}_{-2})=2787.1 m^6/kmol^2.s$$

$$\mathrm{k}_2=4670 m^3/kmol.s$$

And,

$$\frac{1}{\mathrm{k}_2(\mathrm{k}_1/\mathrm{k}_{-2})}=8.63\times 10^{-4} kmol^2.s/m^6$$

Hence,

$$\mathrm{k}_2(\mathrm{k}_1/\mathrm{k}_{-2})=1158.75 m^6/kmol^2.s$$

$$\mathrm{k}_1=8.707 m^3/kmol.s$$

4.1.3 DETERMINING THE RATE COEFFICIENTS AT DIFFERENT TEMPERATURES

Rate coefficients deters at different temperatures. Using the correlations provided by Mandal and Lin, graphs of Figure 6, Figure 7, Figure 8 and Figure 9 are plotted where a linear equation is obtained. Using these linear equations, it is assumed that the blended amine solution exhibits the same trend where more comparison is made using MATLAB.

Figure 6 shows the experimental result by (Lin, 2009) to determine the linear equation for the temperature dependence of k_2 for comparison. It is demonstrated by the graph that the decrease in rate coefficient results in decrease in temperature:

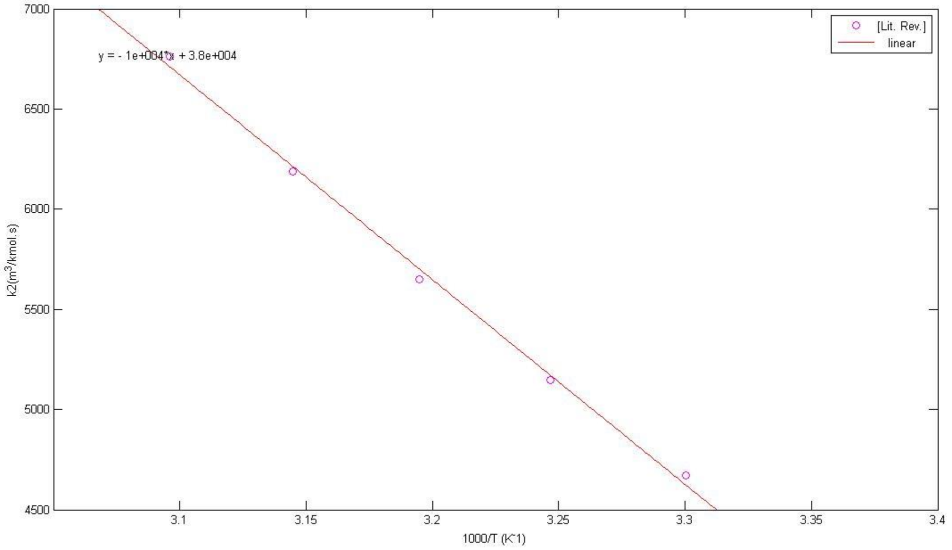

Figure 6: Temperature Dependence of k_2

The linear equation obtained from Figure 6 using MATLAB is shown as below where:

$$y = -1e^4 x + 3.8e^4 \tag{23}$$

Figure 7 shows the experimental result by (Lin, 2009) to determine the linear equation for the temperature dependence of k_1 for comparison. The graph is plotted using k_1 as the x-axis and 1000 $\mathrm{T}^{-1}/\mathrm{K}^{-1}$ as the y-axis. From the graph in Figure 7, it is noticed that the decrease in rate coefficient results in decrease in temperature. From this observation, a linear equation is determined from the line exhibited by the graph.

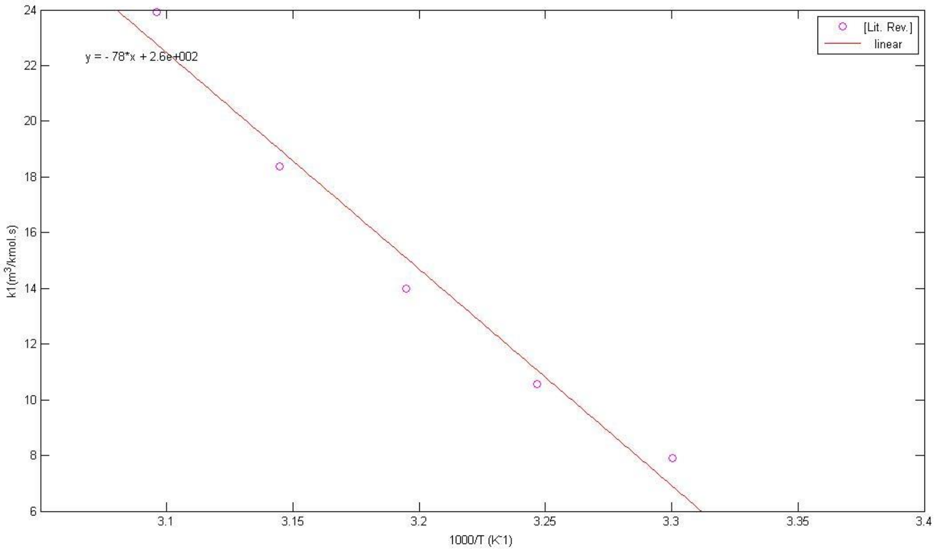

Figure 7: Temperature Dependence of k_1

The linear equation obtained from Figure 7 using MATLAB is shown as below where:

$$y = -78x + 2.6e^{2} \tag{24}$$

Figure 8 shows the experimental result by (Lin, 2009) to determine the linear equation for the temperature dependence of $\mathrm{k}_2(\mathrm{k}_3/\mathrm{k}_{-2})$ for comparison. The graph is plotted using $\mathrm{k}_2(\mathrm{k}_3/\mathrm{k}_{-2})$ as the x-axis and 1000 $\mathrm{T}^{-1}/\mathrm{K}^{-1}$ as the y-axis. From the graph in Figure 8, it is noticed that the decrease in rate coefficient results in decrease in temperature. From this observation, a linear equation is determined from the line exhibited by the graph.

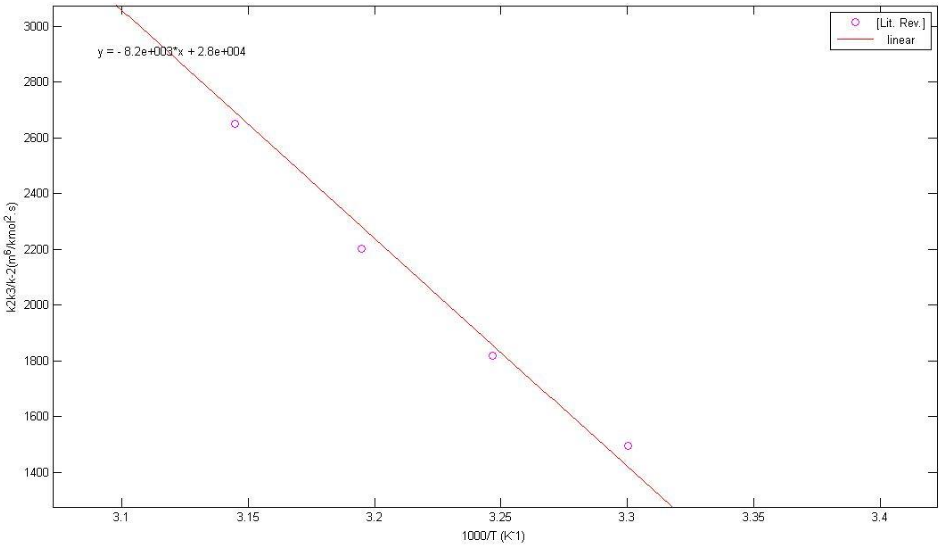

Figure 8: Temperature Dependence of $\mathrm{k}_2(\mathrm{k}_3/\mathrm{k}_{-2})$

The linear equation obtained from Figure 8 using MATLAB is shown as below where:

$$y = -8.2e^3 + 2.8e^4 \tag{25}$$

Figure 9 shows the experimental result by (Lin, 2009) to determine the linear equation for the temperature dependence of $\mathrm{k}_2(\mathrm{k}_1/\mathrm{k}_{-2})$for comparison. The graph is plotted using $\mathrm{k}_2(\mathrm{k}_1/\mathrm{k}_{-2})$as the x-axis and 1000 $\mathrm{T}^{-1}/\mathrm{K}^{-1}$ as the y-axis. From the graph in Figure 9, it is noticed that the decrease in rate coefficient results in decrease in temperature. From this observation, a linear equation is determined from the line exhibited by the graph.

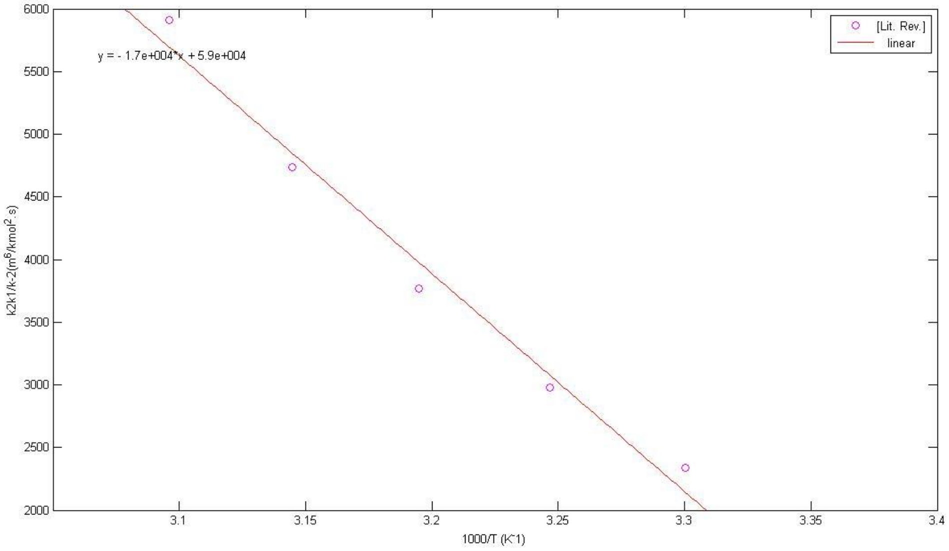

Figure 9: Temperature Dependence of $\mathrm{k}_2(\mathrm{k}_1/\mathrm{k}_{-2})$

The linear equation obtained from Figure 9 using MATLAB is shown as below where:

$$y = -1.7e^4 + 5.9e^4 \tag{26}$$

The linear equation (23) obtained from Figure 6 is then used to plot the graph is Figure 10. This is so that it is assumed that the blended amine solution of MDEA and DEA exhibits the same trend as Figure 6. The rate coefficient of k_2 is obtained and displayed in Table 5. Five different temperatures are chosen which are at 303K, 308K, 313K, 318K and 323K to determine the different rate coefficients. The temperature dependence of k_2 is plotted against 1000 T^{-1}/K^{-1} to compare with the previous Arrhenius plots.

Figure 10 shows the graph is plotted using k_2 as the x-axis and 1000 T^{-1}/K^{-1} as the y-axis. It is demonstrated by the graph that the decrease in rate coefficient results in decrease in temperature of the blended amine solution. From this observation, more accurate values of rate coefficients are obtained and then displayed in Table 5.

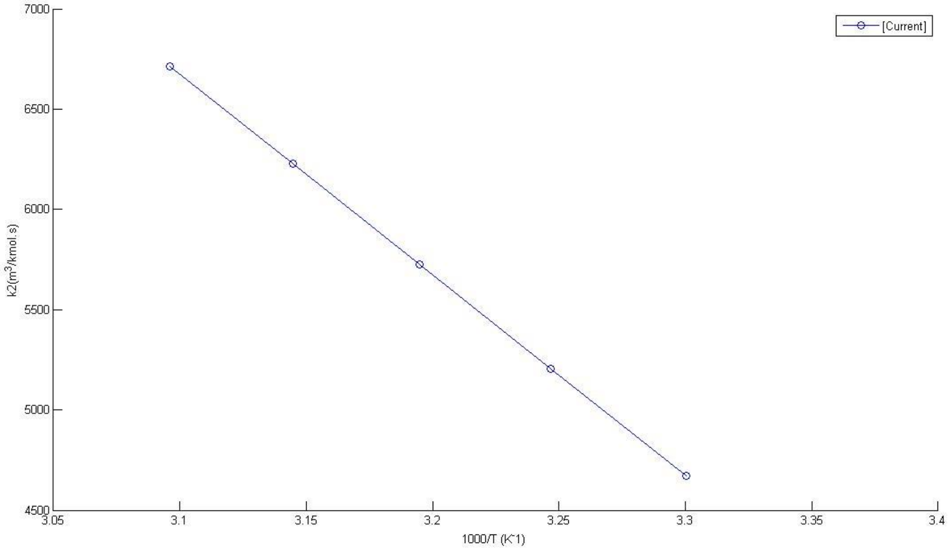

Figure 10: Temperature Dependence of k_2 for blended amine solution

The linear equation (24) obtained from Figure 7 is then used to plot the graph is Figure 11. Reason being, it is assumed that the blended amine solution of MDEA and DEA exhibits the same trend as Figure 7. The rate coefficient of $\mathrm{k_1}$ is obtained and displayed in Table 5. Five different temperatures are chosen which are at 303K, 308K, 313K, 318K and 323K to determine the different rate coefficients. The temperature dependence of $\mathrm{k_1}$ is plotted against 1000 $\mathrm{T^{-1}/K^{-1}}$ to compare with the previous Arrhenius plots.

Figure 11 shows the graph is plotted using $\mathrm{k_1}$ as the x-axis and 1000 $\mathrm{T^{-1}/K^{-1}}$ as the y-axis. It is demonstrated by the graph that the decrease in rate coefficient results in decrease in temperature of the blended amine solution. From this observation, more accurate values of rate coefficients are obtained and then displayed in Table 5.

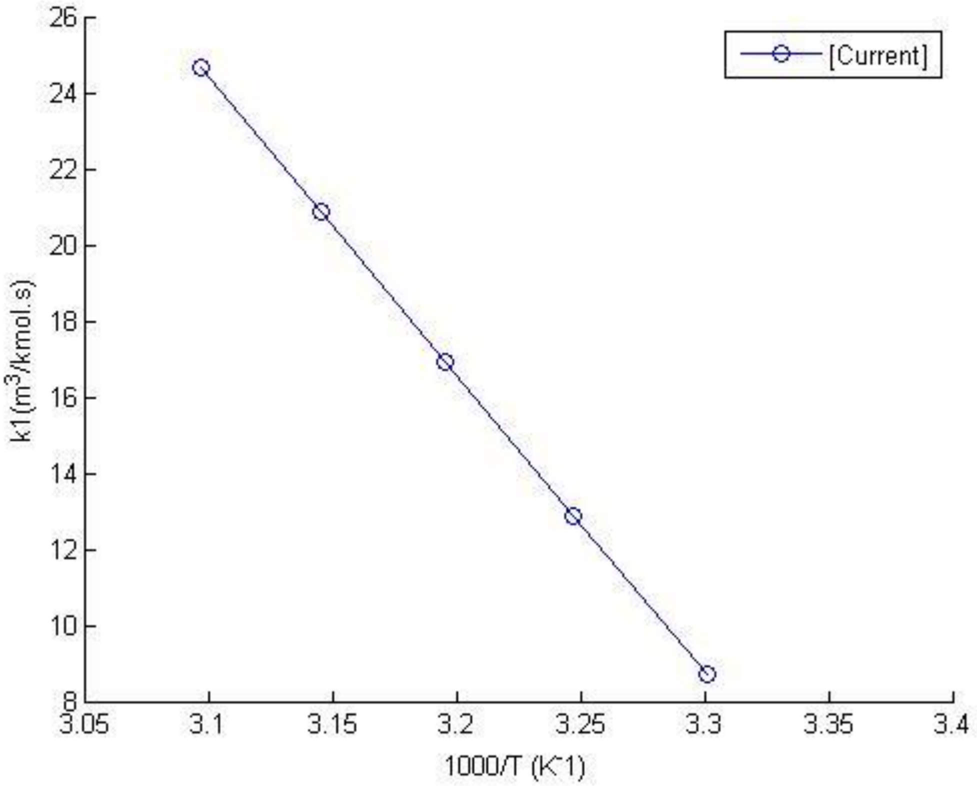

Figure 11: Temperature Dependence of $\mathrm{k_1}$ for blended amine solution

The linear equation (25) obtained from Figure 8 is then used to plot the graph is Figure 12. This is because it is assumed that the blended amine solution of MDEA and DEA exhibits the same trend as Figure 8. The rate coefficient of $k_2(k_3/k_{-2})$ is obtained and displayed in Table 5. Five different temperatures are chosen which are at 303K, 308K, 313K, 318K and 323K to determine the different rate coefficients. The temperature dependence of $k_2(k_3/k_{-2})$ is plotted against $1000\ T^{-1}/K^{-1}$ to compare with the previous Arrhenius plots.

Figure 12 shows the graph is plotted using $k_2(k_3/k_{-2})$ as the x-axis and $1000\ T^{-1}/K^{-1}$ as the y-axis. It is demonstrated by the graph that the decrease in rate coefficient results in decrease in temperature of the blended amine solution. From this observation, more accurate values of rate coefficients are obtained and then displayed in Table 5.

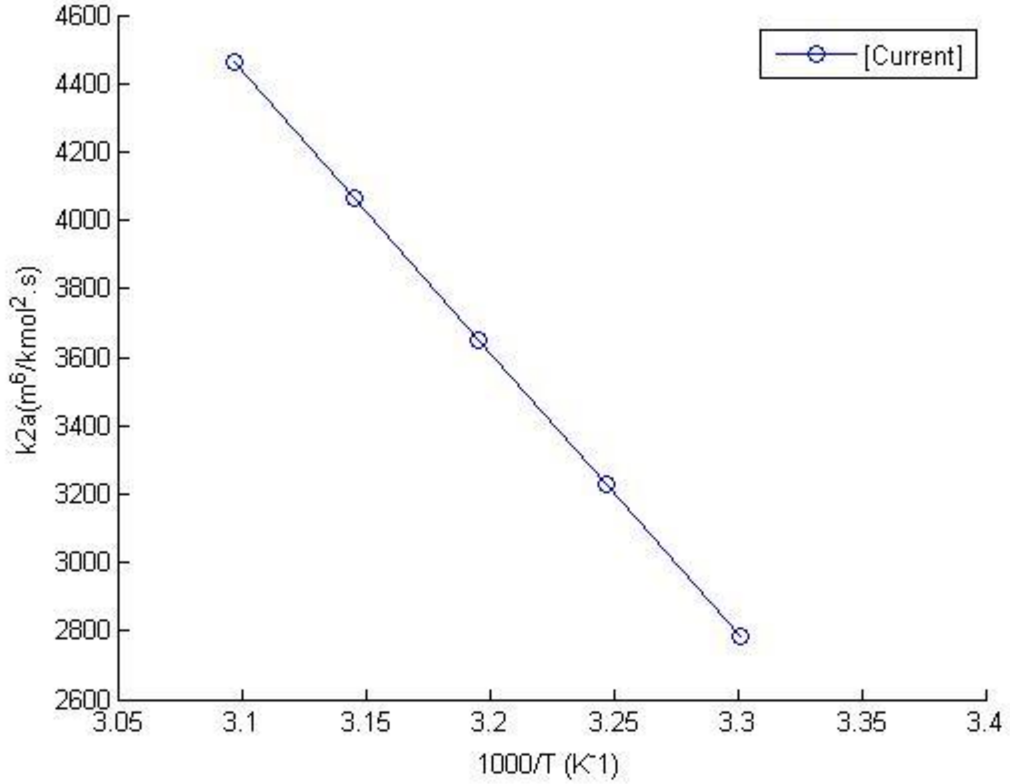

Figure 12: Temperature Dependence of $k_2(k_3/k_{-2})$ for blended amine solution

The linear equation (26) obtained from Figure 9 is then used to plot the graph is Figure 13. Reason being, it is assumed that the blended amine solution of MDEA and DEA exhibits the same trend as Figure 9. The rate coefficient of $\mathrm{k_2(k_1/k_{-2})}$ is obtained and displayed in Table 5. Five different temperatures are chosen which are at 303K, 308K, 313K, 318K and 323K to determine the different rate coefficients. The temperature dependence of $\mathrm{k_2(k_1/k_{-2})}$ is plotted against 1000 $\mathrm{T^{-1}/K^{-1}}$ to compare with the previous Arrhenius plots.

Figure 13 shows the graph is plotted using $\mathrm{k_2(k_1/k_{-2})}$ as the x-axis and 1000 $\mathrm{T^{-1}/K^{-1}}$ as the y-axis. . It is observed from the graph that the decrease in rate coefficient results in decrease in temperature of the blended amine solution. From this observation, more accurate values of rate coefficients are obtained and then displayed in Table 5.

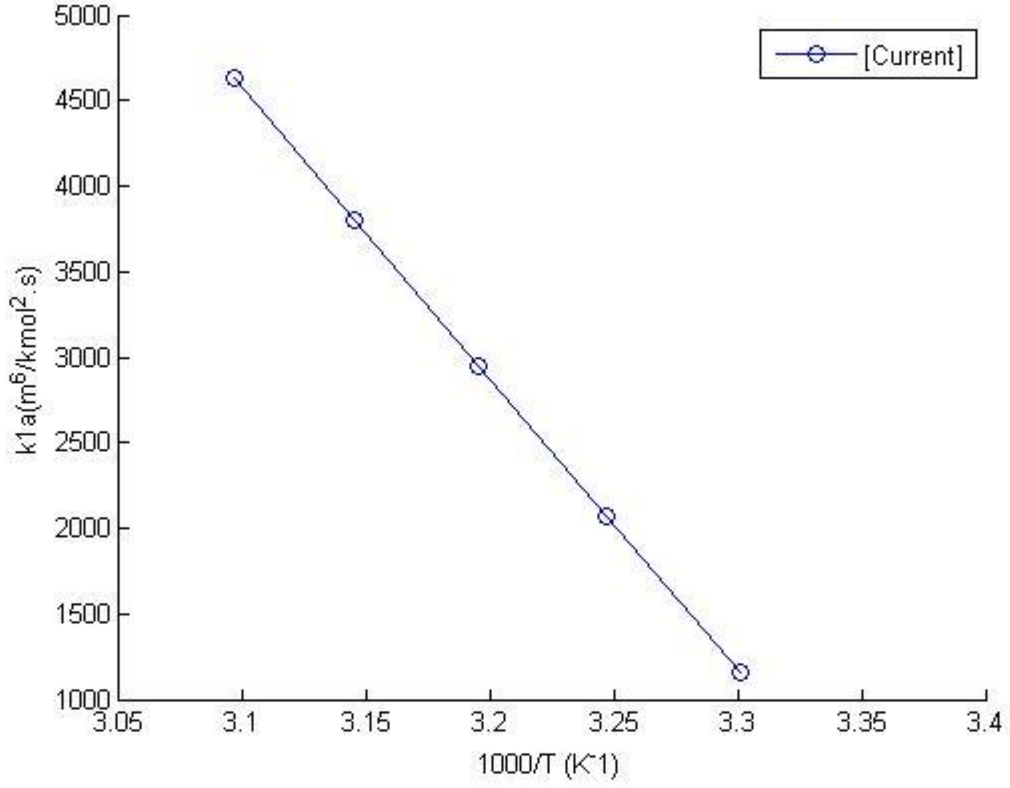

Figure 13: Temperature Dependence of $\mathrm{k_2(k_1/k_{-2})}$ for blended amine solution

4.1.4 PLOTTING THE OBTAINED RATE COEFFICIENTS INTO ARRHENIUS EQUATION

Figure 10- 13 shows how rate coefficients are obtained by plotting the temperature dependence graphs for blended amine solutions. It is plotted by setting rate coefficients as the x-axis and 1000 $\mathrm{T}^{-1}/\mathrm{K}^{-1}$ as the y-axis. Table 5 shows the combine values of rate coefficients obtained from Figures 10-13 for different temperatures of 303K, 308K, 313K, 318K and 323K using MATLAB simulation:

Table 5: Rate coefficient data from MATLAB Simulation

T (K)	k_1 $(m^3/kmol.s)$	k_2 $(m^3/kmol.s)$	$\mathrm{k}_2(\mathrm{k}_1/\mathrm{k}_{-2})$ $(m^6/kmol^2.s)$	$\mathrm{k}_2(\mathrm{k}_3/\mathrm{k}_{-2})$ $(m^6/kmol^2.s)$
303	8.707	4670	1159	2787
308	12.886	5205.8	2069.8	3226.3
313	16.9315	5724.4	2951.5	3651.6
318	20.8497	6226.8	3805.5	4063.5
323	24.6467	6713.5	44633	4462.7

Arrhenius equation is known to be a formula for temperature dependence of reaction rates. It is often used to determine the rate constant, activation energy, temperature or pre-exponential factor of a reaction. The Arrhenius equation is known to be as:

$$\mathrm{k} = \mathrm{A}e^{-\mathrm{E}/\mathrm{RT}}$$

Where,

k = rate constant

A= pre-exponential factor

E= activation energy

R= universal gas constant

T= temperature (K)

The rate coefficients data of difference temperatures from Table 5 are then incorporated into the Arrhenius equation for the determination of the pre-exponential factor and putting the rate constant in terms of the Arrhenius equation. In order to be able to determine the values, the Arrhenius equation has to be derived to form a linear equation. The steps involved in making sure the equation is linear is by taking logs on the left-hand side and right-hand side of the equation. Therefore, the linear equation is known to be as:

$$\mathrm{lnk} = \mathrm{lnA} - \mathrm{E/RT}$$

Incorporating y =mx+c into the above equation:

Gradient, m= $-\mathrm{E/R}$

y-intercept, c= lnA

From the linearized equation, rate coefficients data from Table 5 are used to plot graphs of Figures 14-17 using MATLAB simulation.

Figure 14 shows the graph of linearized Arrhenius equation. In the graph, $\ln k_2$ is used as the x-axis whereas 1/T as the y-axis. Values of k_2 obtained from Table 5 at different temperatures of 303K, 308K, 313K, 318K and 323K are used in order to determine the linear equation which helps in the determination of the pre-exponential factor, A as well as the rate constant equations. The linear equation obtained will then be used using MATLAB simulation in the process of determining the liquid bulk concentration of necessary species.

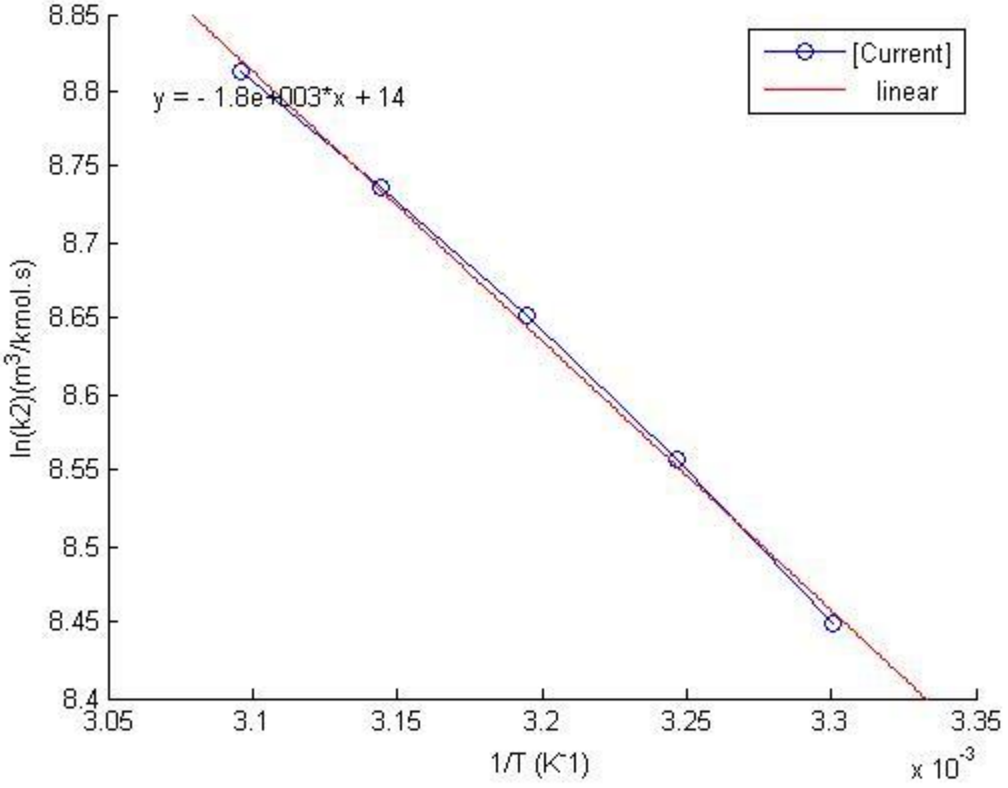

Figure 14: $\ln k_2$ versus 1/T

Calculating for A:

$$\ln A = 14; A = 1.203 \times 10^6$$

Hence,

$$k_2 = 1.203 \times 10^6 e^{(-1800/T)}$$

Figure 15 shows the graph of linearized Arrhenius equation. In the graph, $\ln k_1$ is used as the x-axis whereas 1/T as the y-axis. Values of k_1 obtained from Table 5 at different temperatures of 303K, 308K, 313K, 318K and 323K are used in order to determine the linear equation which helps in the determination of the pre-exponential factor, A as well as the rate constant equations. The linear equation obtained will then be used using MATLAB simulation in the process of determining the liquid bulk concentration of necessary species.

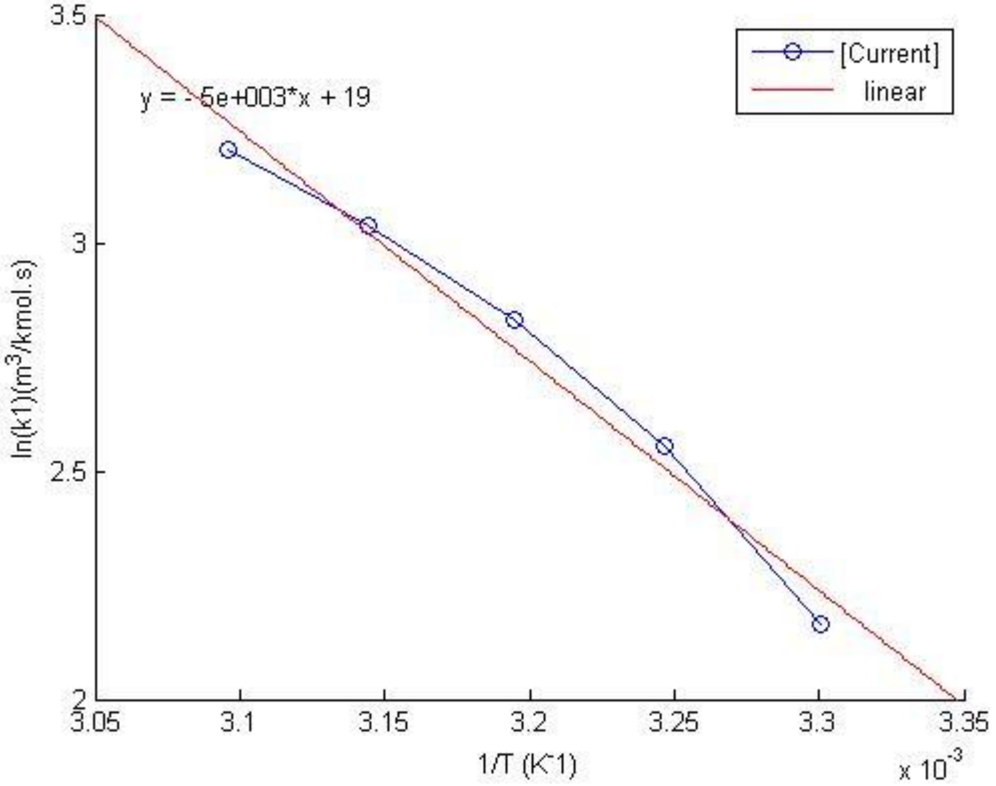

Figure 15: $\ln k_1$ versus 1/T

Calculating for A:

$$\ln A = 19; A = 1.784 \times 10^{8}$$

Hence,

$$k_1 = 1.784 \times 10^{8} e^{(-5000/T)}$$

Figure 16 shows the graph of linearized Arrhenius equation. In the graph, $\ln k_2(k_3/k_{-2})$ is used as the x-axis whereas 1/T as the y-axis. Values of $k_2(k_3/k_{-2})$ obtained from Table 5 at different temperatures of 303K, 308K, 313K, 318K and 323K are used in order to determine the linear equation which helps in the determination of the pre-exponential factor, A as well as the rate constant equations. The linear equation obtained will then be used using MATLAB simulation in the process of determining the liquid bulk concentration of necessary species.

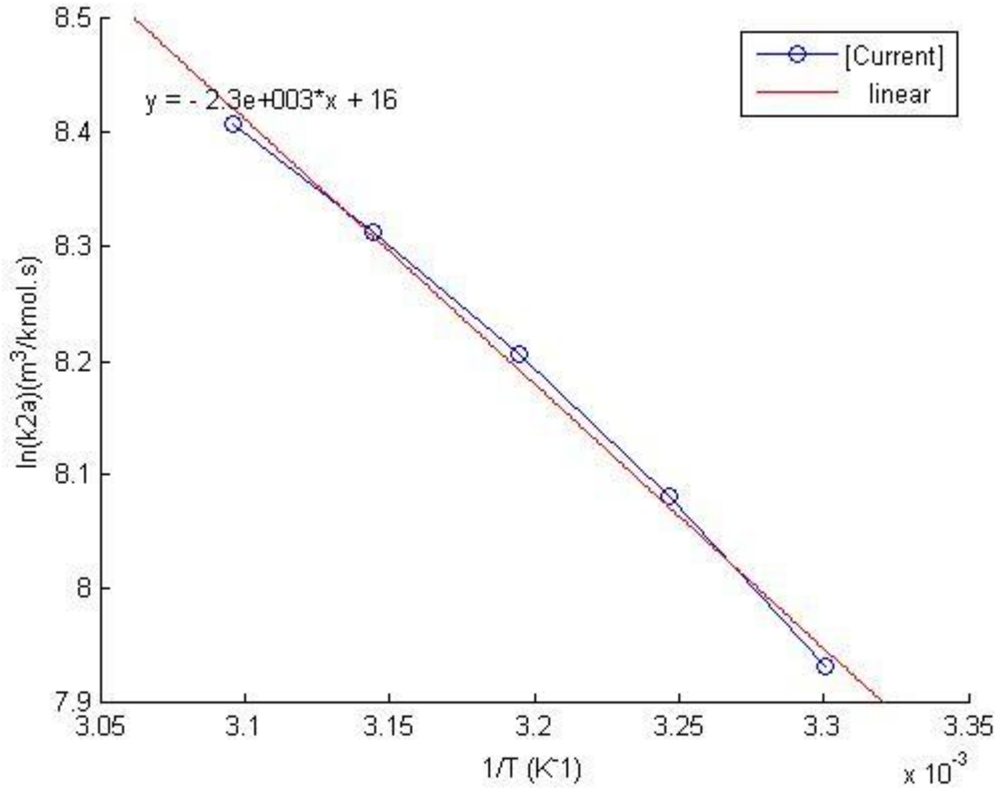

Figure 16: $\ln k_2(k_3/k_{-2})$ versus 1/T

Calculating for A:

$$\ln A = 16; A = 8.886 \times 10^6$$

Hence,

$$k_2(k_3/k_{-2}) = 8.886 \times 10^6 e^{(-2300/T)}$$

Figure 17 shows the graph of linearized Arrhenius equation. In the graph, $\ln k_2(k_1/k_{-2})$ is used as the x-axis whereas 1/T as the y-axis. Values of $k_2(k_1/k_{-2})$ obtained from Table 5 at different temperatures of 303K, 308K, 313K, 318K and 323K are used in order to determine the linear equation which helps in the determination of the pre-exponential factor, A as well as the rate constant equations. The linear equation obtained will then be used using MATLAB simulation in the process of determining the liquid bulk concentration of necessary species.

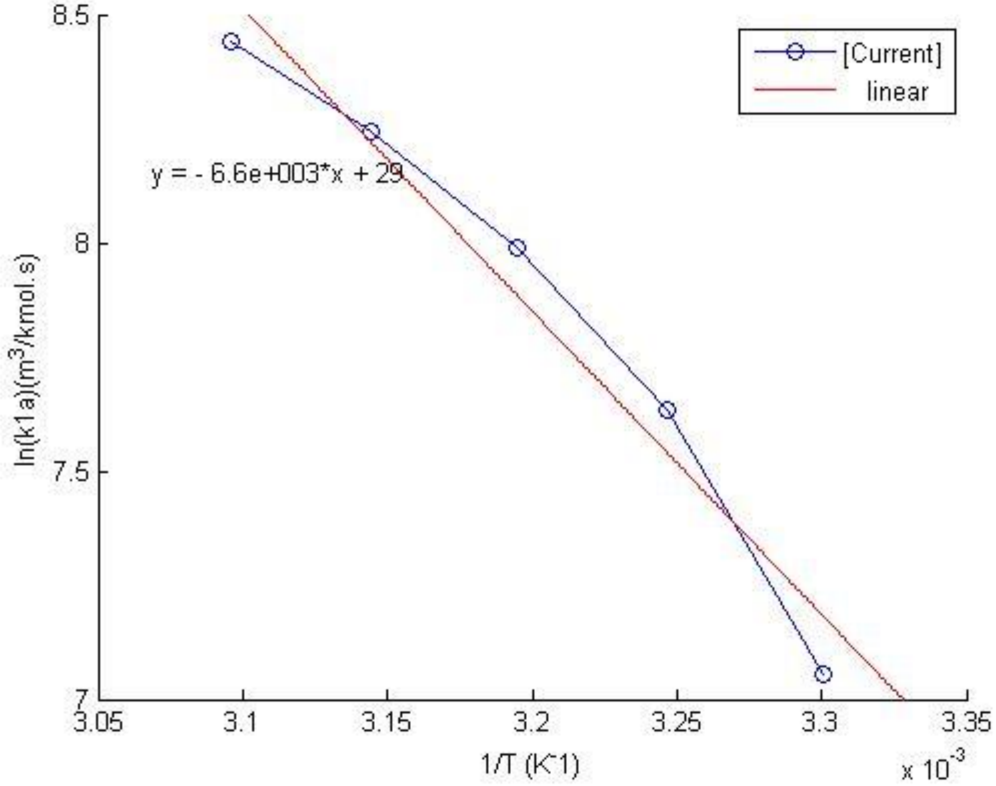

Figure 17: $\ln k_2(k_1/k_{-2})$ versus 1/T

Calculating for A:

$$\ln A = 29; A = 3.931 \times 10^{12}$$

Hence,

$$k_2(k_1/k_{-2}) = 3.931 \times 10^{12} e^{(-6600/T)}$$

4.2 LIQUID BULK CONCENTRATION ESTIMATION

The overall balance of the chemical species are used in order to determine the liquid bulk concentration. There are several assumptions made when simulating the result as shown per below:

1. Initial MDEA concentration to be 1 kmol/m3.
2. Initial DEA concentration to be 1 kmol/m3.
3. Initial carbon dioxide loading to be zero in the solution.

From these assumptions made, equilibrium constant for each reactions using equations of (Lin, 2009) and (Mandal, 2003).

Table 6: Equilibrium Constant

ESTIMATION OF EQUILIBRIUM CONSTANT			
T (K)	303	308	323
K_1	2.981e+005	2.802e+005	2.673+005
$K_2K_3K_9K_{11}$	0	0	0
K_9	5.853e+008	4.445e+008	2.030+008
K_{10}	5.102e-011	5.549e-011	6.681e-011
K_{11}	0	0	0
K_{12}	5.102e-011	5.549e-011	6.681e-011
K_{13}	0	0	0

From Table 6, it can be noticed that the equilibrium constant for reaction (2) and (9) decreases with increasing temperature. It also can be observed that the equilibrium constant for reaction (10) increases with increasing temperature. This phenomenon is exhibited by reaction (12), with increase in temperature, the equilibrium constant increases. As been calculated and simulated in MATLAB, reaction (13) and (11) is related to $K_2K_3K_9K_{11}$thus their values are same throughout at any temperature.

Table 7: Bulk Concentration

LIQUID BULK CONCENTRATION (kmol/m3)				
T (K)	303	308	323	Lit. Rev. (Lin, 2009)
$[R_3N]$	0.999991285	0.999971263	0.999952193	0.995423421
$[R_1R_2NH]$	0.999964115	0.999953901	0.999912787	0.95396730
$[R_1R_2NH_2^+]$	3.58815e-5	5.78345e-5	7.82374e-5	4.56293e-5
$[R_1R_2NCOO^-]$	0	0	0	0
$[CO_2]$	0	0	0	0
$[HCO_3^-]$	0	0	0	0
$[OH^-]$	3.58815e-5	5.78345e-5	7.82374e-5	4.56293e-5
$[CO_3^{2-}]$	0	0	0	0
$[H_3O^+]$	0	0	0	0
$[H_2CO_3]$	0	0	0	0

From Table 7, it is noticed that the initial bulk concentrations of blended amines; MDEA and DEA decreases when the temperature increases to 323K. It is mentioned that the CO2 loading is zero. This directly affects the chemical species which are involved in the carbon dioxide balance equation thus they have zero liquid bulk concentration. The values obtained are then compared to past literature and it is almost similar to those values of (Lin, 2009).

CHAPTER 5: CONCLUSION AND RECOMMENDATION

The use of amines in the removal of carbon dioxide from natural gas has been extensively used in the oil and gas industry. The use of this amine individually has its own drawback. In this case, the use of primary and secondary amine (MEA and DEA) is undesirable as its loading capacity is fixed to a maximum of 0.5 mole of CO2 per mole of amine despite of its high absorption rate (Arthur J. Kidnay, 2006). On the other hand, tertiary amines (MDEA) are able to achieve up to 1 mole of CO2 loading per mole of amine but with a downside of slower absorption rate. To overcome this problem, blends of amine solutions are used as this combines the high absorption capacity of a tertiary amine (MDEA) with the high absorption rates of primary and secondary amine (MEA and DEA) (Zhang et al., 2005). With an incremental of 10% which has been made based on the apparent rate of past literature, new rate coefficients have been determined at different temperatures of 303K, 308K, 313K, 318K and 323K. By determining the Arrhenius plot, linear equations are obtained as well as new rate constants. These values are used to determine the reaction rate kinetics of the solution and with the proposed correlations are modelled using MATLAB. Species of MDEA and DEA is known to decrease with the increasing temperature up to 323K at 0.999952193kmol/m3 of MDEA concentration and 0.999912787kmol/ m3 of DEA concentration. The results simulated as well as calculated shows convincing results when compared to past literature which enables kinetics of CO2 absorption in the blended amine to be known and applied for further study.

To further improve the efficiency of the absorption rate, more parameters should be considered such as various pressures and temperatures of the solutions used. The relationship between CO2 concentrations with the concentration of each amine in the resin should be examined thoroughly by understanding the nature of it so that adequate information and values can be obtained for further improvement to the system. A more complex approach should be employed using MATLAB as well as other software so that comparison can be made to ensure best operating conditions for the solution can be identified.

REFERENCES

Administration, U. S. E. I. (2014). World Energy Consumption, 1990-2035 (Quadrillion Btu). from http://www.eia.gov/forecasts/ieo/ieo_tables.cfm

Ali, W. A. W. A. B. a. R. (2010). *Natural Gas*.

Arthur J. Kidnay, W. R. P. (2006). *Fundamentals of Natural Gas Processing*.

Bereau, U. S. C. (2014). U.S. and World Population Clock. http://www.census.gov/popclock/

Blauwhoff, P. M. M., Versteeg, G. F., & Van Swaaij, W. P. M. (1984). A study on the reaction between CO2 and alkanolamines in aqueous solutions. *Chemical Engineering Science*, *39*(2), 207-225. doi: http://dx.doi.org/10.1016/0009-2509(84)80021-4

Cameron. (2013). Acid Gas CO2 Separation with CYNARA Membranes. *CYNARA CO2 Membrane Separation Solutions*.

Eyton, D. (2014). International Petroleum Week 2014. from http://www.bp.com/en/global/corporate/press/speeches/international-petroleum-week-2014.html

Grande, C. A., & Rodrigues, A. E. (2008). Electric Swing Adsorption for CO2 removal from flue gases. *International Journal of Greenhouse Gas Control, 2*(2), 194-202. doi: http://dx.doi.org/10.1016/S1750-5836(07)00116-8

Ismail, N. B. (2010). Dissertation submitted for the Bachelor of Engineering (Hons) (Chemical Engineering). *Kinetics Modelling of CO2 Reactive Absorption from Natural Gas using MATLAB*

3.

Jerry A. Bullin, J. C. P. a. S. T. D. (1990). *The Use of MDEA and Mixtures of Amines for Bulk CO2 Removal.*

Joel Toreja, B. V., Nelson Chan, John Perry Dickinson. (2011). *Rotary-Valve, Fast-Cycle Pressure-Swing Adsorption Technology Allows West Coast Platform to Meet Tight California Specifications and Recover Stranded Gas.* University of Oklahoma, Norman, Oklahoma.

Kevin M. Lunsford, J. A. B. (1996). Optimization of Amine Sweetening UnitsBryan Research & Engineering, Inc.

Ko, J.-J., & Li, M.-H. (2000). Kinetics of absorption of carbon dioxide into solutions of N-methyldiethanolamine+water. *Chemical Engineering Science*, *55*(19), 4139-4147. doi: http://dx.doi.org/10.1016/S0009-2509(00)00079-8

Kohl, A. L., & Nielsen, R. B. (1997). Chapter 2 - Alkanolamines for Hydrogen Sulfide and Carbon Dioxide Removal. In A. L. Kohl & R. B. Nielsen (Eds.), *Gas Purification (Fifth Edition)* (pp. 40-186). Houston: Gulf Professional Publishing.

Liao, C.-H., & Li, M.-H. (2002). Kinetics of absorption of carbon dioxide into aqueous solutions of monoethanolamine+N-methyldiethanolamine. *Chemical Engineering Science*, *57*(21), 4569-4582. doi: http://dx.doi.org/10.1016/S0009-2509(02)00395-0

Lin, C.-Y., Soriano, A. N., & Li, M.-H. (2009). Kinetics study of carbon dioxide absorption into aqueous solutions containing N-methyldiethanolamine+diethanolamine. *Journal of the Taiwan Institute of Chemical Engineers*, *40*(4), 403-412. doi: 10.1016/j.jtice.2008.11.002

Yan, S., Fang, M., Zhang, W., Zhong, W., Luo, Z., & Cen, K. (2008). Comparative analysis of CO2 separation from flue gas by membrane gas absorption technology and chemical absorption technology in China. *Energy Conversion and Management*, *49*(11), 3188-3197. doi: http://dx.doi.org/10.1016/j.enconman.2008.05.027

Zhang, X., Schubert, S., Gruenewald, M., & Agar, D. W. (2005). Studies on the kinetics of carbon dioxide absorption with immobilised amines (IA). *Chemical Engineering Journal*, *107*(1–3), 97-102. doi: http://dx.doi.org/10.1016/j.cej.2004.12.015

APPENDICES

Appendix 1: Figure 2

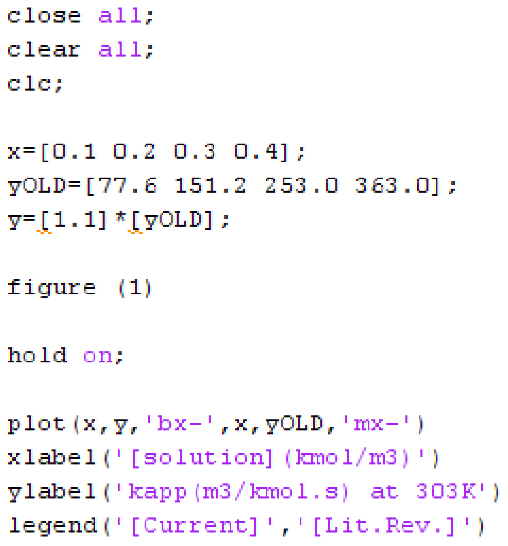

```
close all;
clear all;
clc;

x=[0.1 0.2 0.3 0.4];
yOLD=[77.6 151.2 253.0 363.0];
y=[1.1]*[yOLD];

figure (1)

hold on;

plot(x,y,'bx-',x,yOLD,'mx-')
xlabel('[solution](kmol/m3)')
ylabel('kapp(m3/kmol.s) at 303K')
legend('[Current]','[Lit.Rev.]')
```

Appendix 2: Figure 3

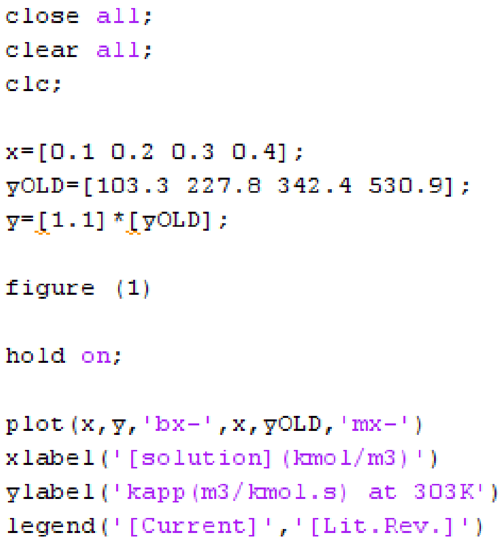

```
close all;
clear all;
clc;

x=[0.1 0.2 0.3 0.4];
yOLD=[103.3 227.8 342.4 530.9];
y=[1.1]*[yOLD];

figure (1)

hold on;

plot(x,y,'bx-',x,yOLD,'mx-')
xlabel('[solution](kmol/m3)')
ylabel('kapp(m3/kmol.s) at 303K')
legend('[Current]','[Lit.Rev.]')
```

Appendix 3: Figure 4

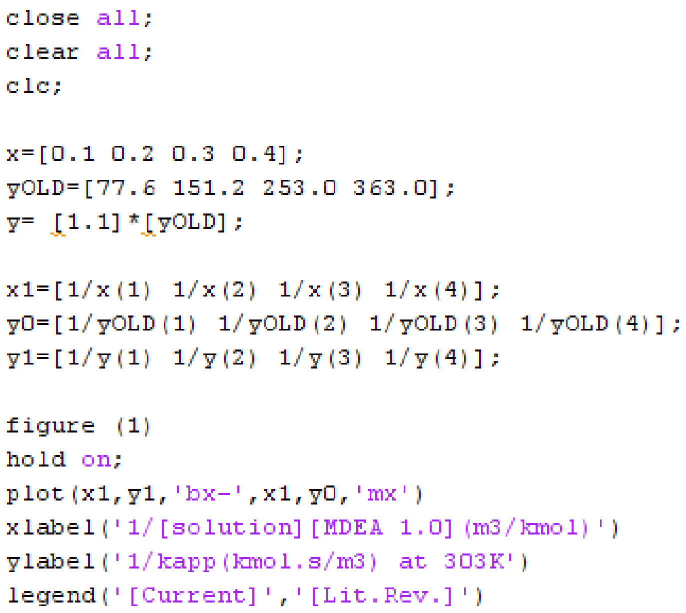

```
close all;
clear all;
clc;

x=[0.1 0.2 0.3 0.4];
yOLD=[77.6 151.2 253.0 363.0];
y= [1.1]*[yOLD];

x1=[1/x(1) 1/x(2) 1/x(3) 1/x(4)];
y0=[1/yOLD(1) 1/yOLD(2) 1/yOLD(3) 1/yOLD(4)];
y1=[1/y(1) 1/y(2) 1/y(3) 1/y(4)];

figure (1)
hold on;
plot(x1,y1,'bx-',x1,y0,'mx')
xlabel('1/[solution][MDEA 1.0](m3/kmol)')
ylabel('1/kapp(kmol.s/m3) at 303K')
legend('[Current]','[Lit.Rev.]')
```

Appendix 4: Figure 5

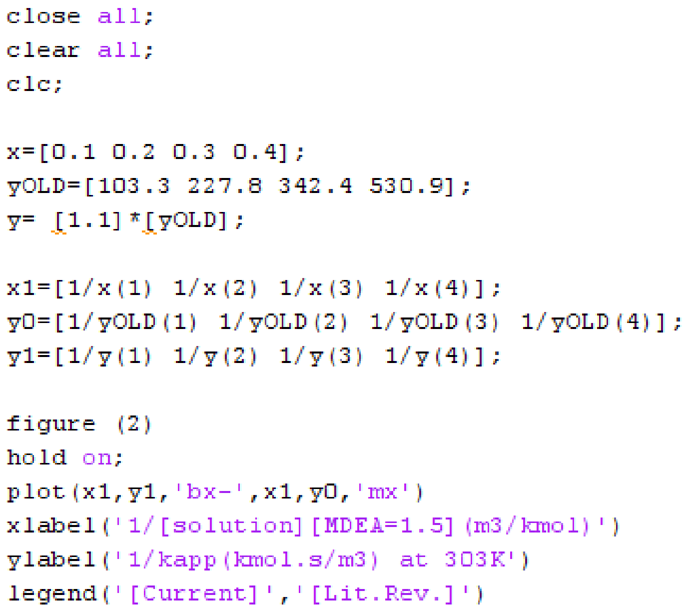

```
close all;
clear all;
clc;

x=[0.1 0.2 0.3 0.4];
yOLD=[103.3 227.8 342.4 530.9];
y= [1.1]*[yOLD];

x1=[1/x(1) 1/x(2) 1/x(3) 1/x(4)];
y0=[1/yOLD(1) 1/yOLD(2) 1/yOLD(3) 1/yOLD(4)];
y1=[1/y(1) 1/y(2) 1/y(3) 1/y(4)];

figure (2)
hold on;
plot(x1,y1,'bx-',x1,y0,'mx')
xlabel('1/[solution][MDEA=1.5](m3/kmol)')
ylabel('1/kapp(kmol.s/m3) at 303K')
legend('[Current]','[Lit.Rev.]')
```

Appendix 5: Figure 6 and 8

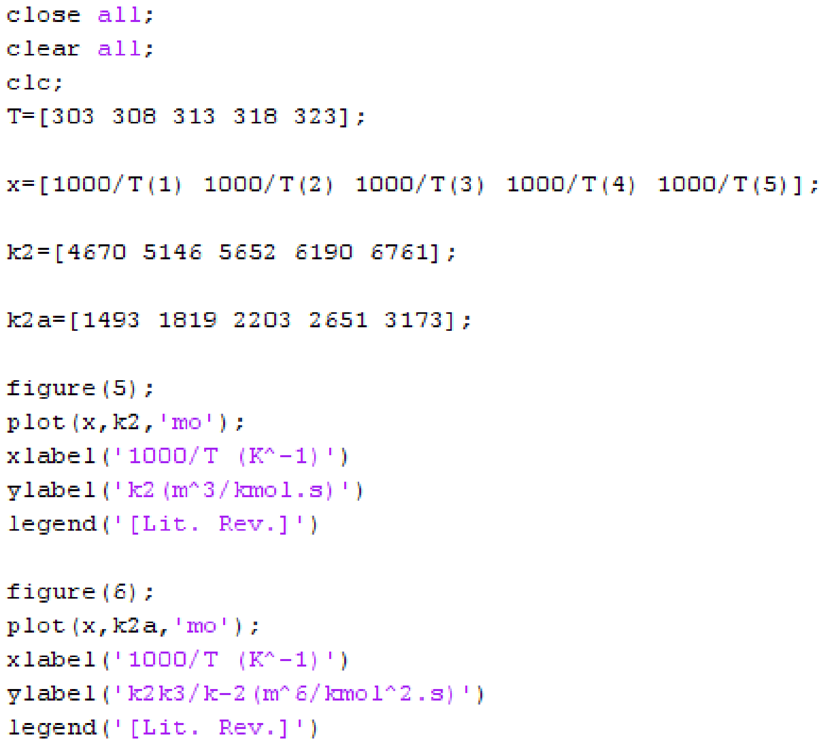

```
close all;
clear all;
clc;
T=[303 308 313 318 323];

x=[1000/T(1) 1000/T(2) 1000/T(3) 1000/T(4) 1000/T(5)];

k2=[4670 5146 5652 6190 6761];

k2a=[1493 1819 2203 2651 3173];

figure(5);
plot(x,k2,'mo');
xlabel('1000/T (K^-1)')
ylabel('k2(m^3/kmol.s)')
legend('[Lit. Rev.]')

figure(6);
plot(x,k2a,'mo');
xlabel('1000/T (K^-1)')
ylabel('k2k3/k-2(m^6/kmol^2.s)')
legend('[Lit. Rev.]')
```

Appendix 6: Figure 7 and 9

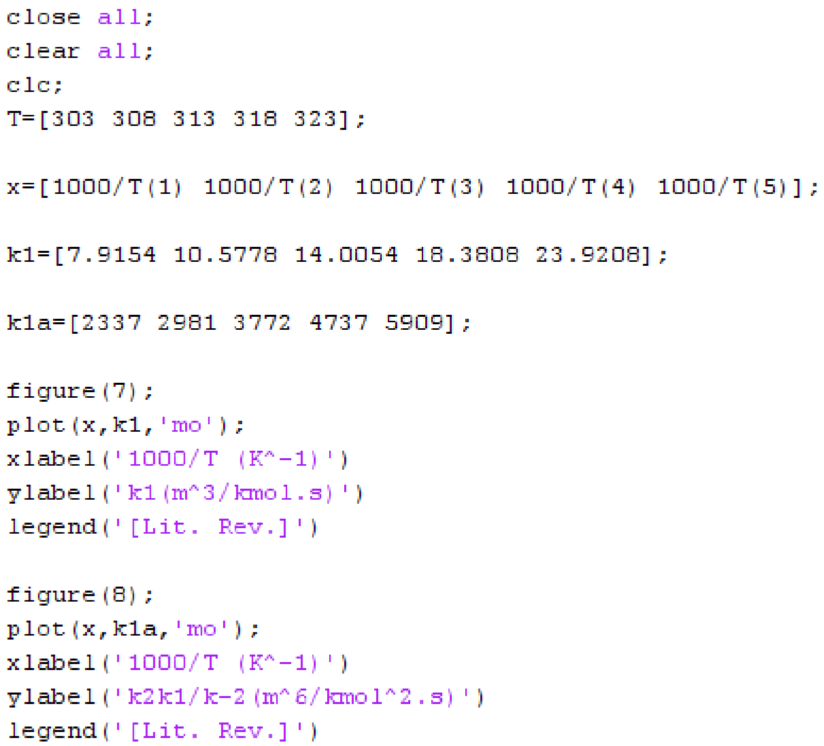

```
close all;
clear all;
clc;
T=[303 308 313 318 323];

x=[1000/T(1) 1000/T(2) 1000/T(3) 1000/T(4) 1000/T(5)];

k1=[7.9154 10.5778 14.0054 18.3808 23.9208];

k1a=[2337 2981 3772 4737 5909];

figure(7);
plot(x,k1,'mo');
xlabel('1000/T (K^-1)')
ylabel('k1(m^3/kmol.s)')
legend('[Lit. Rev.]')

figure(8);
plot(x,k1a,'mo');
xlabel('1000/T (K^-1)')
ylabel('k2k1/k-2(m^6/kmol^2.s)')
legend('[Lit. Rev.]')
```

Appendix 7: Figure 10

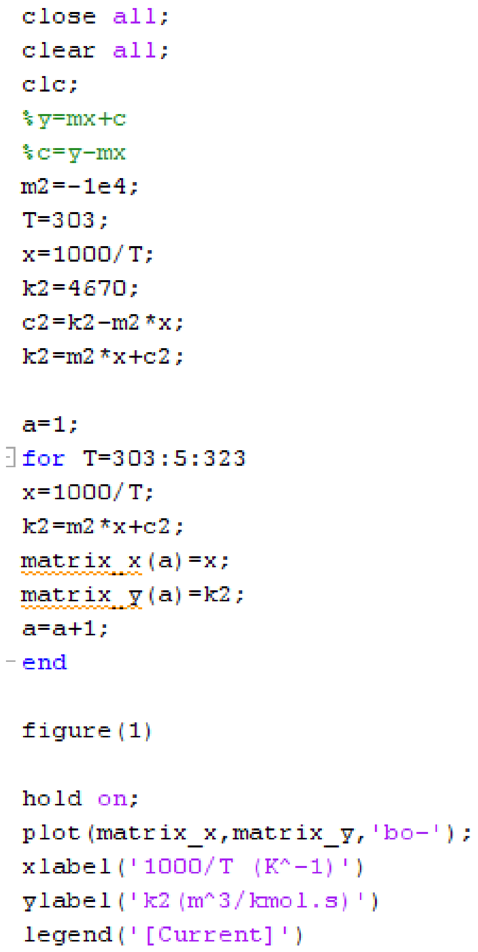

```
close all;
clear all;
clc;
%y=mx+c
%c=y-mx
m2=-1e4;
T=303;
x=1000/T;
k2=4670;
c2=k2-m2*x;
k2=m2*x+c2;

a=1;
for T=303:5:323
x=1000/T;
k2=m2*x+c2;
matrix_x(a)=x;
matrix_y(a)=k2;
a=a+1;
end

figure(1)

hold on;
plot(matrix_x,matrix_y,'bo-');
xlabel('1000/T (K^-1)')
ylabel('k2(m^3/kmol.s)')
legend('[Current]')
```

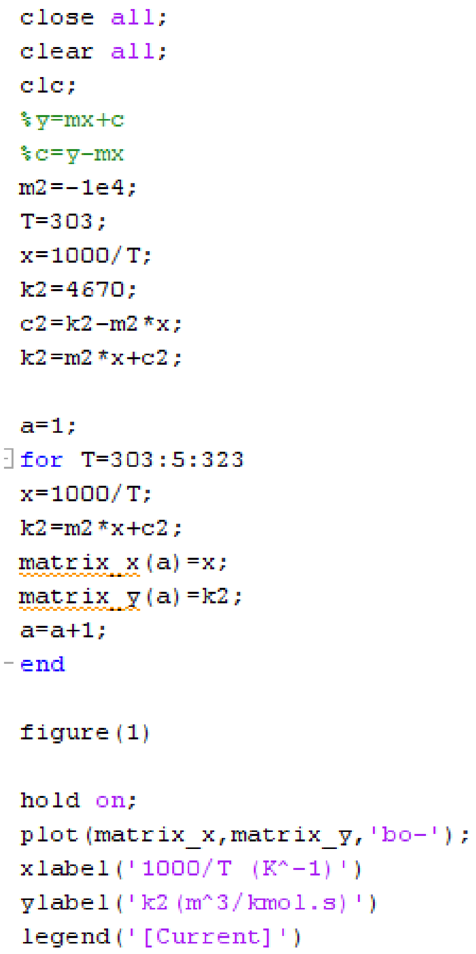

```
close all;
clear all;
clc;
%y=mx+c
%c=y-mx
m2=-1e4;
T=303;
x=1000/T;
k2=4670;
c2=k2-m2*x;
k2=m2*x+c2;

a=1;
for T=303:5:323
x=1000/T;
k2=m2*x+c2;
matrix_x(a)=x;
matrix_y(a)=k2;
a=a+1;
end

figure(1)

hold on;
plot(matrix_x,matrix_y,'bo-');
xlabel('1000/T (K^-1)')
ylabel('k2(m^3/kmol.s)')
legend('[Current]')
```

Appendix 10: Figure 11

```
close all;
clear all;
clc;
%y=mx+c
%c=y-mx
m1=-78;
T=303;
x=1000/T;
k1=8.707;
c1=k1-m1*x;
k1=m1*x+c1;

a=1;
for T=303:5:323
x=1000/T;
k1=m1*x+c1;
matrix_x(a)=x;
matrix_y(a)=k1;
a=a+1;
end

figure(1)

hold on;
plot(matrix_x,matrix_y,'bo-');
xlabel('1000/T (K^-1)')
ylabel('k1(m^3/kmol.s)')
legend('[Current]')
```

Appendix 11: Figure 12

```
close all;
clear all;
clc;
%y=mx+c
%c=y-mx
m2a=-8.2e3;
T=303;
x=1000/T;
k2a=2787;
c2a=k2a-m2a*x;
k2a=m2a*x+c2a;

a=1;
for T=303:5:323
x=1000/T;
k2a=m2a*x+c2a;
matrix_x(a)=x;
matrix_y(a)=k2a;
a=a+1;
end

figure(1)

hold on;
plot(matrix_x,matrix_y,'bo-');
xlabel('1000/T (K^-1)')
ylabel('k2a(m^6/kmol^2.s)')
legend('[Current]')
```

Appendix 12: Figure 13

```
close all;
clear all;
clc;

m1a=-1.7e4;
T=303;
x=1000/T;
k1a=1159;
c1a=k1a-m1a*x;
k1a=m1a*x+c1a;

a=1;
for T=303:5:323
x=1000/T;
k1a=m1a*x+c1a;
matrix_x(a)=x;
matrix_y(a)=k1a;
a=a+1;
end

figure(1)

hold on;
plot(matrix_x,matrix_y,'bo-');
xlabel('1000/T (K^-1)')
ylabel('k1a(m^6/kmol^2.s)')
legend('[Current]')
```

Appendix 13: Figure 14

```
close all;
clear all;
clc;
m2=-1e4;
T=303;
x=1000/T;
k2=4670;

c2=k2-m2*x;
k2=m2*x+c2;

a=1;
for T=303:5:323
x=1000/T;
t=1/T;
k2=m2*x+c2;
lnk2=log(k2);
matrix_x(a)=x;
matrix_y(a)=k2;
matrix_t(a)=t;
matrix_lnk2(a)=lnk2;
a=a+1;
end

figure(1)
hold on;
plot(matrix_t,matrix_lnk2,'bo-');
xlabel('1/T (K^-1)')
ylabel('ln(k2)(m^3/kmol.s)')
legend('[Current]')
```

Appendix 14: Figure 15

```
close all;
clear all;
clc;

m1=-78;
T=303;
x=1000/T;
k1=8.707;

c1=k1-m1*x;
k1=m1*x+c1;

a=1;
for T=303:5:323
x=1000/T;
t=1/T;
k1=m1*x+c1;
lnk1=log(k1);
matrix_x(a)=x;
matrix_y(a)=k1;
matrix_t(a)=t;
matrix_lnk1(a)=lnk1;
a=a+1;
end

figure(1)
hold on;
plot(matrix_t,matrix_lnk1,'bo-');
xlabel('1/T (K^-1)')
ylabel('ln(k1)(m^3/kmol.s)')
legend('[Current]')
```

Appendix 15: Figure 16

```
close all;
clear all;
clc;

m1a=-1.7e4;
T=303;
x=1000/T;
k1a=1159;

c1a=k1a-m1a*x;
k1a=m1a*x+c1a;

a=1;
for T=303:5:323
x=1000/T;
t=1/T;
k1a=m1a*x+c1a;
lnk1a=log(k1a);
matrix_x(a)=x;
matrix_y(a)=k1a;
matrix_t(a)=t;
matrix_lnk1a(a)=lnk1a;
a=a+1;
end

figure(1)
hold on;
plot(matrix_t,matrix_lnk1a,'bo-');
xlabel('1/T (K^-1)')
ylabel('ln(k1a)(m^3/kmol.s)')
legend('[Current]')
```

Appendix 16: Figure 17

```
close all;
clear all;
clc;

m1a=-1.7e4;
T=303;
x=1000/T;
k1a=1159;

c1a=k1a-m1a*x;
k1a=m1a*x+c1a;

a=1;
for T=303:5:323
x=1000/T;
t=1/T;
k1a=m1a*x+c1a;
lnk1a=log(k1a);
matrix_x(a)=x;
matrix_y(a)=k1a;
matrix_t(a)=t;
matrix_lnk1a(a)=lnk1a;
a=a+1;
end

figure(1)
hold on;
plot(matrix_t,matrix_lnk1a,'bo-');
xlabel('1/T (K^-1)')
ylabel('ln(k1a)(m^3/kmol.s)')
legend('[Current]')
```

Appendix 17: Equilibrium Constant Estimation

```
function BulkConcentrationBlendedAmine
T=input('Enter T value: ');

k1=0.026 %s-1,at 25oCslow

%log10K13 = 13.635 - (2895/T)
log10K13= 13.635 - (2895/T);
k13=10^(log10K13)

%log10(1/K9) = -4.0302 - (1830.15/T) + 0.0043*T
log10lovrK9 = -4.0302 - (1830.15/T) + 0.0043*T;
K9=1/(10^(log10lovrK9))

%log10K10 = 6.498 - 0.0238*T - (2902.4/T)
log10K10 = 6.498 - 0.0238*T - (2902.4/T);
K10=10^(log10K10)

%log10(1/K11) = 8909.483 - (142613.6/T) - 4229.195*log10(T) + 9.7384*T
- 0
log10lovrK11 = 8909.483 - (142613.6/T) - 4229.195*log10(T) + 9.7384*T -
0;
K11=1/(10^(log10lovrK11))

%K13--
log10K13ovrK11 = 179.648 + (0.019244*T) - 67.341*log10(T) + 7495.441/T
;K13ovrK11=10^(log10K13ovrK11)
K13=K13ovrK11*K11

%K1--
log10K3ovrK11 = (-7261.78/T) -22.4773*log(T) + 142.58612;
K3ovrK11=10^(log10K3ovrK11)
K1=K13*K3ovrK11

%calculation for K2K3---
k2=1.203E6*exp(-1800/T);

%K2K3=k2k3k2r
k2k3k2r=8.886E6*exp(-2300/T);
K2K3=8.886E6*exp(-2300/T)

%calculation for K2K3K9K11
K2K3K9K11=K2K3*K9*K11

%no correlation found to fit K12, thus:
K12=K10 %assumption
%-------------------------------------------------------------------
T
K1
K2K3K9K11
K9
K10
K11
```

```
K12
K13
%-----------------------------------------------------------------

S = solve ('Cco + Cdo + Ceo - 1 = 0 ','Cfo + Cgo + Cio + Ceo + Cko =
0','Cdo + Cjo - Cgo - Cho - (2*Cio) -Ceo + Cbo = 0','Cgo -
(0*(Cfo*Cho)) = 0','(Cjo*Ceo) - (0*(Cfo*Cco)) = 0','Cco-
(7.7668e+008*(Cdo*Cho)) = 0','Cio - (4.6345e-011*(Cgo*Cho)) = 0','Cko -
(4.6345e-011*(Cgo*Cjo)) = 0','(Cho*Cjo) = 0')
Cf1o=S.Cf1o;
Cco=S.Cco;
Cdo=S.Cdo;
Cgo=S.Cgo;
Cho=S.Cho;
Cio=S.Cio;
Cjo=S.Cjo;
Ceo=S.Ceo;
Cko=S.Cko;
Cfo=S.Cfo(2)
Cco=S.Cco(2)
Cdo=S.Cdo(2)
Cgo=S.Cgo(2)
Cho=S.Cho(2)
Cio=S.Cio(2)
Cjo=S.Cjo(2)
Ceo=S.Ceo(2)
Cko=S.Cko(2)
```